

TUFTS UNIVERSITY DEPARTMENT OF BIOMEDICAL ENGINEERING

# Silk Microsphere Encapsulation of Wound Healing Peptides for Regenerative Medicine

---

Senior Honors Thesis

Katerina Kovalenko

5/1/2011

## **Acknowledgements**

I would like to thank my advisor, Dr. Ira Herman, for his guidance in developing and conducting this project. I would also like to thank Dr. David Kaplan for his support throughout and his readiness to answer questions and make suggestions. I am also grateful to Dr. Tatiana Demidova-Rice for her help developing and conducting the *in vitro* tube proliferation studies as well as planning the *in vivo* studies. Additionally, a special thank you to Dr. Eleanor Pritchard for teaching me how to make microspheres and for providing invaluable guidance on the materials aspects of the project. Finally, I would like to thank my family and Stephen Wilson for their love and support throughout this challenging process.

## Table of Contents

<b>Table of Figures.....</b>	<b>vi</b>
<b>Abbreviations.....</b>	<b>vii</b>
<b>Abstract.....</b>	<b>1</b>
<b>Background and Introduction.....</b>	<b>2</b>
<i>I. Wound Healing.....</i>	<i>3</i>
<i>II. Existing Strategies in Chronic Wound Care.....</i>	<i>4</i>
<i>III. UN3 and Comb1 Development and Research.....</i>	<i>5</i>
<i>IV. Silk for Drug Delivery.....</i>	<i>7</i>
<i>V. Controlled Release Drug Delivery Systems.....</i>	<i>8</i>
<i>VI. The Tube Formation Assay.....</i>	<i>9</i>
<b>Hypothesis.....</b>	<b>10</b>
<b>Specific Aims.....</b>	<b>11</b>
<b>Methods.....</b>	<b>13</b>
<i>I. Peptide Isolation.....</i>	<i>13</i>
A. Materials.....	13
B. Isolation and Characterization.....	13
<i>i) UN3.....</i>	<i>13</i>
<i>ii) Comb1.....</i>	<i>13</i>
<i>II. Formation of Silk Microspheres.....</i>	<i>14</i>
A. Materials.....	14
B. Microsphere Construction.....	15

i) Silk Purification.....	15
ii) Microsphere Formation.....	15
iii) Microsphere Processing.....	16
III. ELISA Development.....	16
A. Materials.....	16
B. Standard Curve Development.....	16
i) Biotinylated-Comb1 ELISA.....	17
ii) UN3 ELISA.....	17
IV. Release Studies.....	19
A. Materials.....	19
B. Fourteen-day Release Studies.....	19
i) FITC- Comb1.....	19
ii) Biotinylated-Comb1 and UN3.....	20
iii) Peptide Loss and Total Peptide Content Quantification.....	20
C. Quantification of Peptide.....	20
V. Cell Studies.....	20
A. Materials.....	21
B. Tube Proliferation Studies.....	21
i) Tube Proliferation Study in Eight-Well Chamber Slides.....	21
ii) Tube Proliferation Study in 24-Well Transwell Plate.....	22
VI. Statistical Analysis.....	22

<b>Results.....</b>	<b>24</b>
<i>I. Release Profile</i>	
<i>Study.....</i>	<i>24</i>
<i>II. Protein</i>	
<i>Loss.....</i>	<i>28</i>
<i>III. ELISA Optimization Study.....</i>	<i>29</i>
<i>IV. Tube Proliferation Assay.....</i>	<i>31</i>
<b>Discussion.....</b>	<b>41</b>
<b>Conclusions.....</b>	<b>46</b>
<b>Future Work.....</b>	<b>47</b>
<b>Literature Cited.....</b>	<b>viii</b>

## Figures and Tables

Table i. Abbreviations used throughout the paper.....	vi
Table 1. Standard curves constructed for UN3 ELISA development.....	18
Figure 1. Cumulative mass release of biotinylated-Comb1, FITC-Comb1 and UN3 from 1mg microspheres.....	24
Figure 2. Cumulative mass release of new and old FITC-Comb1 from 1 mg microspheres.....	25
Figure 3. Cumulative mass release of new and old biotinylated-Comb1 from 1 mg microspheres.....	26
Figure 4. Cumulative mass release of new and old UN3 from 1 mg microspheres.....	27
Table 2. Cumulative percent of initially added peptide that is released.....	28
Table 3. Distribution of initial FITC-Comb1 during microsphere formation and processing.....	29
Figure 5. Standard curves of biotinylated-Comb1 diluted in DPBS obtained by ELISA.....	29
Figure 6. Standard curves of UN3 diluted in DPBS obtained by ELISA.....	30
Figure 7. Quantitative evaluation of tube proliferation on chamber slides six hours post-plating.....	31
Figure 8. Photomicrographs of capillary-like structures formed by CEC on chamber slides six hours post-plating.....	32
Figure 9. Quantitative evaluation of tube proliferation on chamber slides 23 hours post-plating.....	34
Figure 10. Photomicrographs of capillary-like structures formed by CEC on chamber slides 23 hours post-plating.....	35
Figure 11. Quantitative evaluation of tube proliferation on a transwell plate slides five hours post-plating.....	36
Figure 12. Photomicrographs of capillary-like structures formed by CEC on a transwell plate five hours post-plating.....	38
Figure 13. Quantitative evaluation of tube proliferation on a transwell plate slides 23 hours post-plating.....	39
Figure 14. Photomicrographs of capillary-like structures formed by CEC on a transwell plate 23 hours post-plating.....	40

## Abbreviations

<b>Table i. Abbreviations used throughout the paper (alphabetical order)</b>	
<b>Abbreviation</b>	<b>Meaning</b>
BComb1	biotinylated-Comb1
BREC	bovine retinal endothelial cell
CEC	capillary endothelial cell
CMC	carboxymethyl cellulose
DOPC	1,2-Dioleoyl- <i>sn</i> -Glycero-3-Phosphocholine
ECM	extracellular matrix
EGF	endothelial growth factor
EGTA	ethylene glycol tetraacetic acid
FComb1	FITC-Comb1
Fn	fibronectin
FNIII29	fibronectin type III repeat 29
GFR	growth factor reduced
HFIP	hexafluoroisopropanol
KO	knock-out
mTNX	mouse tenascin X
PBS	phosphate-buffered saline
PDGF	platelet-derived growth factor
SDS	sodium dodecyl sulfate
TNX	tenascin X
TUCF	Tufts University Core Facility
VEGF	vascular endothelial growth factor
VEGFR-1	vascular endothelial growth factor receptor 1

## Abstract

Chronic wounds are comorbid with diseases that are on the rise, such as diabetes mellitus and atherosclerosis, and as such present a growing problem to the medical community. Although there is a range of treatment options available, from hyperbaric oxygen treatments to tissue grafts, there has been an increasing interest in the use of bioactive peptides, specifically those involved in angiogenesis, for the treatment of chronic wounds. In accordance with this, two peptides were developed in the Herman laboratory – UN3 and Comb1. UN3 is a peptide isolated from platelet releasate, whereas Comb1 is a combinatorial peptide synthesized from the EGF-like domains of fibrillin 1 and tenascin X, two noncollagenous ECM peptides. Both of these peptides have been shown to stimulate angiogenesis *in vitro*. However, in order to facilitate controlled and predictable release of the peptides they were tested in a silk microsphere drug delivery system. This system has the benefits of being biocompatible and biodegradable, undergoes processing under ambient conditions, and can be modified to change drug delivery rates. In this study, preliminary evaluations of the release profile of biotinylated-Comb1, FITC-Comb1, and UN3 from silk microspheres were performed, and the bioactivity of the peptides after they were released was assessed with an *in vitro* tube formation study. It was found that all three peptides showed a characteristic release profile that fit a logarithmic regression curve with high correlation, and that silk microsphere delivery was more efficient for FITC-Comb1 and biotinylated-Comb1 than UN3. It was also shown *in vitro* that silk microspheres loaded with the angiogenic peptides stimulated significantly greater angiogenesis than the serum control at the seven hour time point, as measured by total tube proliferation. Future work should focus on conducting *in vivo* studies with the silk microsphere drug delivery system and in optimizing the microspheres for more sustained release.

## Background and Introduction

With a growing population of the elderly and a rise in the level of diabetes mellitus, atherosclerosis and venous insufficiency among adults in the US, the incidence of chronic wounds associated with these disorders has also risen over the last few decades (Tatsioni *et al*, 2007). Chronic wounds, characterized by an incapability of the epithelium to return to its former state of structural and functional integrity, are a highly destructive affliction. They are usually very painful, disruptive to the patient's lifestyle, and create a large cost burden both on each individual patient and on the healthcare system as a whole. They also often lead to amputation, an outcome which is not only highly undesirable but which also correlates with an increased mortality rate among patients (Page, 2002). Devising an effective treatment for chronic wounds is therefore a public health priority and a serious engineering challenge that must be addressed.

There is currently a large amount of interest in the development of bioactive peptides for the treatment of chronic wounds. Two such peptides, UN3 and Comb1, were developed by the Herman laboratory (Sackler School, Tufts University) and demonstrated to have significant angiogenic properties both *in vitro* and *in vivo*. Since angiogenesis is a crucial component of the wound healing process and one that chronic wound patients are often deficient in, these peptides represent an exciting opportunity in chronic wound care. However, as with any drug, these peptides require a drug delivery system which will safely and effectively deliver its burden to a target location. It is also important for a drug delivery system to be convenient, as this minimizes the ever-present issue of patient non-compliance. In view of these requirements, this project focused on exploring silk microspheres as a drug delivery system for UN3 and Comb1. Silk is an excellent material for drug delivery because it is both biocompatible and biodegradable, which minimizes the risk of adverse reactions and obviates the need to later remove the

drug delivery system from the patient's body. In addition, microspheres provide a good format for drug delivery in this context, because they demonstrate a predictable release profile over time, which means that the drug can be administered less often, they are stable, they can be synthesized under relatively mild conditions which prevent the peptide being encapsulated from being denatured, and they are lyophilized and stored, meaning that they protect peptides that are sensitive to being in solution such as Comb1 (Dr. Tatiana Demidova-Rice, personal communication). Therefore, establishing the release profiles and bioactivity of Comb1 and UN3 in the context of silk microsphere encapsulation is an important step in developing these peptides into a viable clinical treatment for chronic wounds.

### *1. Wound Healing*

Normal wound healing is a complex process that requires a well-orchestrated series of physiological events, including cell migration and proliferation, extracellular matrix deposition and remodeling, as well as the influx of inflammatory molecules, cytokines, and growth factors. The process of wound repair falls roughly into four overlapping categories, namely coagulation, inflammation, migration-proliferation and remodeling (Falanga, 2005). Coagulation and inflammation are mainly characterized by plugging the wound with platelets in a meshwork of fibrin followed by wound debridement by inflammatory cells such as neutrophils and macrophages. Hypoxia in the wound at this stage is necessary, as it activates keratinocyte migration. Migration-proliferation and remodeling, on the other hand, involve wound contraction as well as formation of extracellular matrix proteins (Falanga, 2005). Angiogenesis plays an important role in the second half of wound healing by supplying all cells at the wound site with oxygen, nutrients, and cytokines. Angiogenesis itself is dependent on the recruitment of endothelial progenitor cells from circulation and on the sprouting of resident endothelial cells from the edge of the wound. This sprouting is in turn stimulated by growth factors released by platelets, macrophages and keratinocytes such as vascular endothelial growth factor (VEGF) and

platelet-derived growth factor (PDGF). It is also dependent on the extracellular matrix of the wound environment, which serves both as a scaffold and which releases pro- and antiangiogenic factors upon degradation by scaffold-remodeling enzymes like collagenases, matrix metalloproteinases, and serine proteases (Demidova-Rice *et al*, 2011). Therefore, a combinatory peptide composed of two proangiogenic factors (Comb1) and another peptide isolated from platelet releasate (UN3) were chosen for their angiogenic properties to be further tested in a silk microsphere delivery system.

## *II. Existing Strategies in Chronic Wound Care*

Standard clinical care for chronic wounds currently includes either surgical or enzymatic wound debridement, as well as cleansing, dressings (occlusive, semi-occlusive and non-occlusive), compression bandages, the use of antibiotics, and pressure offloading (Tatsioni *et al*, 2007). In addition to these standard practices, a number of other treatments are available for chronic wounds. Some options for non-bioactive treatment include hyperbaric oxygen therapy, which relies on exposure to 100% oxygen at an increased pressure in order to stimulate neovascularization, collagen production, and PDGF synthesis. There is also electrical stimulation therapy, which increases blood flow, decreases edema, inhibits bacterial growth, and has been shown to increase the synthesis of PDGF, as well others that use ultrasound, radiant heat warming, and negative pressure (Page 2002). Most of these techniques aim to reduce edema and increase circulation to the site, since low levels of blood flow are a large contributor to chronic wounds.

The three main bioactive approaches to chronic wound healing are keratinocyte cultures, tissue replacements, and growth factors. For keratinocyte cultures, an autogenic graft is grown *in vitro* and then applied to the wound. The drawbacks of this technique are that it is relatively costly, that the graft is fragile and thus needs to be applied with a synthetic backing such as silicone, and that it takes approximately three weeks to grow the necessary amount of tissue to cover the wound, during which

time a temporary covering of cadaver or porcine skin is used. This approach makes sense for patients who have lost a large surface area of skin, such as burn victims, but the cost and time delay are hard to justify for smaller wounds (Page 2002). A similar strategy consists of growing allogeneic tissue replacements in the laboratory using keratinocytes for the epidermal layer and a mixture of neonatal fibroblasts and bovine collagen for the dermis. Because neonatal fibroblasts are not highly immunogenic, rejection has not been a problem. Clinical trials of these tissue replacement constructs have shown up to a 49% improvement in chronic wound healing (Page 2002).

The third type of bioactive wound healing currently under investigation examines the use of growth factors. The two high profile growth factor solutions are Procuren and Regranex. Procuren is based on an autologous platelet releasate that contains a mixture of growth factors. The solution was found to be effective, especially in patients with deep wounds. However, it had to be applied daily, and it had to be made individually for each patient because it relied on their own blood for platelet isolation. In addition, it turned out to not be economically viable and was removed from the US market. The second growth factor solution, Regranex, is an FDA-approved gel containing a PDGF-BB isoform. This gel must be applied daily to the wound, but has shown a 43% increase in wound healing compared to controls in clinical trials (Page 2002).

The peptides examined in this study act on a similar principle as Regranex. UN3 is derived from platelet releasate, and Comb1 is composed of EGF-like domains of ECM fragments. Although data for UN3 is not available, Comb1 has been shown to induce almost doubling in the total length of sprout produced in a Matrigel tube proliferation assay (Demidova-Rice *et al*, 2011). Because of these promising results *in vitro* it was chosen, along with UN3, for testing with the silk microsphere drug delivery system.

### *III. UN3 and Comb1 Development and Research*

UN3 is a peptide that was isolated and identified from platelet releasates using size exclusion, ion chromatography and mass spectrometry. Its amino acid sequence is ELLESYIDTRPTATSEYQTFNPR (Dr. Tatiana Demidova-Rice, personal communication). Unpublished data obtained in the laboratory of Dr. Ira Herman (Sackler School, Tufts University) demonstrate that this peptide stimulates cellular responses to injury both *in vitro* and *in vivo*. *In vivo* delivery in mice was performed using a carboxymethyl cellulose delivery system (Dr. Tatiana Demidova-Rice, personal communication). Due to the sensitive nature of the unpublished material, no further information on the peptide is available at this time.

Comb1 is a 25 amino acid long synthetic peptide with the sequence DINECEIGAPAGEETEVTVEGLEPG derived from the limited digestion of the bovine retinal endothelial cell (BREC) extracellular matrix (ECM) with bacterial collagenase from *Clostridium histolyticum*. This peptide is combinatorial, consisting of fragments of EGF-like domains from tenascin X and fibrillin 1, two noncollagenous proteins (Demidova-Rice *et al*, 2011). Fibrillin 1 is a large extracellular matrix glycoprotein that is a structural component of 10-12 nm calcium-binding microfibrils, which provide support in connective tissue throughout the body (NCBI 2011). It has also been shown to stabilize blood vessels *in vivo*, with mouse mutants for that gene showing increased levels of aneurism (Sottile 2004). It has been shown that fibrillin 1 mediates cell adhesion and binds to purified integrin  $\alpha V\beta 3$  via an RGD sequence (Pfaff *et al*, 1996), which sustains angiogenesis (Demidova-Rice *et al*, 2011).

Tenascin X is an extracellular matrix glycoprotein that is thought to function in matrix maturation during wound healing (NCBI 2011). Tenascin X was first isolated by Bristow *et al* (1993) as a new protein containing a series of fibronectin (Fn) type III repeats, endothelial growth factor (EGF)-like repeats, as well as a globular domain shared with the fibrinogens like the rest of the tenascin family, although the specific number of repeats varies among members. Tenascin X is highly expressed in heart

and skeletal muscle as well as around blood vessels (Tomoki *et al*, 2000). Experiments in mice have shown that mouse tenascin X (mTNX) binds to VEGF-B and enhances its ability to stimulate cell proliferation by increasing the signals mediated by the VEGFR-1 receptor, suggesting that TNX plays a role in angiogenesis (Tomoki *et al*, 2000). In their analysis of the role of TNX in wound healing in mice, Egging *et al* (2008) found that TNX was expressed at very low levels in the wounds of wild type mice seven days after wounding, but started to be expressed at moderate levels after 14 days post-wounding. They showed that the mechanical strength of the wild type scars was comparable to the scars of mice that were KO for TNX at seven days, but that after 14 days the wild type scars had further increased their breaking strength, whereas the KO scar breaking strength did not supersede the KO uninjured breaking strength (Egging *et al*, 2008). This suggested that TNX is involved in establishing the biomechanical properties of the ECM through remodeling and maturation rather than matrix deposition. Thus, the tenascin X protein is believed to be involved in wound healing through its interactions with VEGF-B, which help stimulate angiogenesis, as well as its role in matrix stabilization, remodeling and maturation.

Comb1 was chosen for this study due to its angiogenic properties. Demidova-Rice *et al* (2011) demonstrated that Comb1 induces a significant increase in endothelial proliferation and a two-fold increase in *in vitro* angiogenesis when compared to a 1% DMEM control. In that study, which compared a number of degradation products from the ECM of CECs, all of which were immunoprecipitated with antibodies against collagen I-V, Comb1 was shown to be one of the best stimulants of angiogenesis. In view of this, it makes a promising candidate for the treatment of chronic wounds because it is capable of helping to reestablish the vasculature of the wound, the insufficiency of which is often the cause of difficulty healing.

#### *IV. Silk for Drug Delivery*

In recent years silk and silk-derived proteins have been increasingly examined for their potential use in medical treatments. Silk proteins are attractive in this context as they are self-assembling and have minimal effect on the body, being both biocompatible and biodegradable. It is relatively easy to control certain physical properties of silk such as solubility and shape. Early efforts yielded silk-based sutures, currently an FDA certified material, but present work has a greater emphasis on the pharmaceutical and biotechnological applications (Numata *et al*, 2010).

The challenge facing modern drug delivery is to develop the capacity to administer medication in a precisely controlled quantity, within a certain time, onto a specified target area. The controlled release of pharmaceutically active compounds is an area of particular interest as it reduces the number of doses required to treat patients, thus minimizing the issue of patient non-compliance, and provides a more stable effect. Silk has the potential to be very useful in this application as its biocompatibility and biodegradability minimize the risk of harmful side effects that sometimes result from drug delivery methods, while its strong physical properties make it capable of mechanically protecting the active compound prior to delivery (Numata *et al*, 2010). Thus, silk was chosen as the medium for drug delivery of the peptides being tested because of its capacity for sustained release and because of its low impact on the patient.

#### *V. Controlled Release Drug Delivery Systems*

Silk morphology is highly customizable, resulting in a wide variety of structures including microspheres, films, and nanoparticles. Silk microspheres are constructed by encapsulating lipid micelle templates in silk and then removing the lipid with methanol treatment. Microspheres are especially useful for drug delivery given their ability to fully encase the active compound and a relatively slow degradation rate. Microspheres typically have an average diameter of approximately three micrometers, making them well sized for the delivery of small molecules (Numata *et al*, 2010). They can be further optimized by manipulating  $\beta$ -sheet content to adjust the degradation rate (Wenk *et al*,

2010). Such a high level of customizability, combined with the favorable physical and biological properties gives silk microspheres a strong potential for use in drug delivery.

Another advantage of silk-based drug delivery systems like microspheres over competing drug delivery systems such as poly(D,L-lactide-co-glycolide) (PLGA) and natural polymers such as collagen and alginate is that silk can be processed at ambient conditions. This obviates the need for high temperatures or organic solvents which may damage or denature the protein to be delivered. Silk processing conditions also allow for better modulation of the release profile, making such drug delivery systems even more useful (Wang *et al*, 2007). In view of these advantages, silk microspheres were chosen as the drug delivery system for this experiment.

#### *VI. The Tube Formation Assay*

The tube formation assay is based on plating capillary endothelial cells on Matrigel, a sterilized tumor extract that is biologically active and contains all of the components present in the basement membrane. Matrigel has become a popular model for angiogenesis because it promotes differentiation *in vitro*. Its particular effect on endothelial cells is that it stimulates them to form capillary tubes with lumen (Kleinman and Martin, 2005). This simulates endothelial cell migration and capillary formation *in vivo*, and is therefore a useful assay to predict the effect of drugs on angiogenesis much more easily and cheaply than is possible in an *in vivo* study. In this paper, the tube formation assay was used to determine whether peptides released from a silk microsphere drug delivery system were bioactive and as capable of stimulating angiogenesis as before encapsulation.

## Hypothesis

In this study, we constructed silk microspheres loaded with FITC-Comb1, biotinylated-Comb1, and UN3. We hypothesized that these microspheres would release the peptides over the course of approximately two weeks and create a defined release profile, as characterized by detection and quantification of peptide in a DPBS release assay. We further hypothesized that the peptides, thus encapsulated and released, would retain their bioactivity, as determined by an *in vitro* tube proliferation assay. Finally, we hypothesized that an ELISA could be developed to quantify concentrations of biotinylated-Comb1 and UN3 in solution.

## Specific Aims

The main objectives of this research were:

1) *To study and compare the release profiles of the microsphere constructs loaded with FITC-Comb1, biotinylated-Comb1, and UN3.* The objective of this aim was to determine the two-week release profile of FITC-Comb1, biotinylated-Comb1, and UN3 from silk. To address this aim, silk microspheres were loaded with 0.1mg/mL of each peptide and then a release study in DPBS was performed over a two-week period. The amount of peptide released was quantified using either a fluorescence assay or an ELISA, and fit to a regression curve in order to define a release profile for each peptide. This aim was achieved when the release profile of each peptide was fitted to a regression curve with high correlation.

2) *To determine the bioactivity of FITC-Comb1, biotinylated-Comb1, and UN3 after they are released from the silk microspheres.* The objective of this aim was to determine that FITC-Comb1, biotinylated-Comb1, and UN3 retain their bioactivity upon release from the microspheres. Since these peptides are temperature sensitive, it was important to establish that they were not denatured or otherwise inactivated by the process of microsphere formation. To address this aim, both naked and encapsulated peptides were added to capillary endothelial cells cultured on Matrigel and the capillary-like tube formation in these cells was quantified. This aim was achieved when the tube formation stimulated by the encapsulated peptides was found to be statistically significantly higher than a serum-stimulated control.

3) *To optimize ELISA reagent concentrations in order to accurately assay biotinylated-Comb1 and UN3 in solution.* The objective of this aim was to develop a protocol to quantify the concentration of biotinylated-Comb1 and UN3 in solution using ELISA, since no such protocol existed. To address this aim,

serial dilutions of biotinylated-Comb1 were assayed with an ELISA using streptavidin-HRP conjugate concentrations of 1.0  $\mu\text{g}/\text{mL}$  and 0.5  $\mu\text{g}/\text{mL}$  to determine which would yield a regression curve with a higher correlation coefficient. Similarly, serial dilutions of UN3 were assayed with an ELISA using unpurified primary antibody concentrations of 0.5, 1.0, 5.0, 10, 20, 30, 50, 100 and 200  $\mu\text{g}/\text{mL}$ , and purified secondary HRP-goat anti-rabbit IgG dilutions of 1:10000, 1:3000, 1:1000 and 1:500 to determine which yielded a regression curve with the highest correlation coefficient. This aim was achieved when the standard curve produced by the assays of serial dilutions of biotinylated-Comb1 and UN3 fit a linear and logarithmic regression curve, respectively, with high correlation.

## Methods

### *I. Peptide Isolation*

#### A. Materials

Bovine capillary endothelial cells were isolated and provided by the Herman laboratory. Purified Clostridial collagenase was obtained from Advance Biofactures (Lynbrook, NY). Protease inhibitors and 2-mercaptoethanol were obtained from Sigma-Aldrich (St. Louis, MO). Collagen I antibody as well as mixed collagen I-V antibodies were ordered from Abcam (Cambridge, MA). Protein A sepharose was obtained from GE Healthcare (Uppsala, Sweden).

#### B. Isolation and Characterization

##### *i) UN3*

UN3 is a peptide derived from human platelet releasates using size exclusion, ion chromatography and mass spectrometry (Dr. Tatiana Demidova-Rice, personal communication). This peptide was purified and kindly provided by the Herman laboratory for the experiments described below. The amino acid sequence of the final product was determined to be ELLESYIDTRPTATSEYQTFNPR. Further information on this peptide is not currently available due to the sensitive nature of the unpublished material.

##### *ii) Comb1*

Comb1 is a peptide derived from the ECM of bovine endothelial capillary cells, as described previously (Demidova-Rice *et al*, 2011). It was synthesized and kindly provided by the Herman laboratory for the experiments discussed below. Briefly, CECs isolated and stored in liquid nitrogen by the Herman

laboratory were cultured and washed three times with PBS (pH 7.15) 7-10 days postconfluence. Cells were then removed with 0.5% sodium deoxycholate buffered with 20 mM Tris-Cl (pH 8.0) with 15 mM NaCl, 1 mM EGTA (pH 7.0) and 1 mM phenylmethyl sulfonyl fluoride. The matrix was then washed with PBS and immediately collected. Enzymatic degradation of the matrix was carried out with purified Clostridial collagenase, which was stored at 1 mg/mL in 1 M Tris-HCl (pH 7) at -20°C and diluted in calcium-buffered saline at 16 U/mL immediately before use, and then added to the plates of ECM for one hour at 37°C. Matrices were then scraped into 0.1x immunoprecipitation buffer containing 0.125% bovine serum albumin, 30mM Tris-Cl (pH 8), 0.1% sodium dodecyl sulfate (SDS), 0.5% sodium deoxycholate, 1% NP-40, and protease inhibitors, lyophilized overnight and reconstituted in one tenth the volume of distilled water. ECM was precleared with protein A sepharose in the absence of antibody. Immunoprecipitation was carried out using either anti-collagen I antibody or a mix of anti-collagen I-V antibodies. Protein A sepharose beads were washed three times in distilled water and suspended in immunoprecipitation buffer with protease inhibitors. Antibodies were added at 225 mg/mL and incubated with agitation for one hour at room temperature to allow them to bind to the beads. Precleared ECM was added to the beads and incubated at 4°C overnight with rotation. Proteins were then eluted using boiling SDS containing 2% 2-mercaptoethanol, subject to gel electrophoresis and stained with Coomassie blue dye. Protein bands were excised, washed twice with 50% acetonitrile and identified at Tufts University Core Facility (TUCF), where they were degraded with proteomics-grade trypsin and subjected to liquid chromatography mass spectrometry. The combination of fibrillin 1 and tenascin X fragments that made up Comb1 was chosen to be synthesized via FastMoc Chemistry at TUCF. The amino acid sequence of the final product was DINECEIGAPAGEETEVTVEGLEPG (Demidova-Rice *et al*, 2011).

## *II. Formation of Silk Microspheres*

## A. Materials

*Bombyx mori* silk cocoons were obtained from Tajima Shoji Co., Ltd (Sumiyoshicho, Naka-ku, Yokohama, Japan). All chemicals were purchased from Sigma-Aldrich (St. Louis, MO).

## B. Microsphere Construction

### *i) Silk Purification:*

*Bombyx mori* cocoons were cut into dime-sized pieces and 5 g was boiled in 2 L of 20 mM sodium carbonate for 30 minutes. The silk fibroin was then washed in excess distilled H<sub>2</sub>O three times for twenty minutes each time. The fibroin was pulled apart by hand, spread out and left to dry overnight at room temperature. The silk fibroin was dissolved in 9.3 M LiBr at 60°C for four hours to make a 20% (w/v) solution. The silk solution was loaded into Slide-a-Lyzer 3-12 mL dialysis cassettes (MWCO 3,500, Pierce) and dialyzed against 1 L distilled water per cassette in order to remove LiBr. Dialysis water was changed six times over the course of two days in order to maintain a favorable concentration gradient. The solution was removed from the cassettes, placed into Falcon tubes and centrifuged in a fixed-angle rotator at 8°C and 5000rpm for thirty minutes to remove any debris. The concentration of the silk solution was found by drying a known volume of solution via evaporation and obtaining the mass of the product. Silk solution concentration was brought above 8% (w/v) by loading the silk solution into 3-12 mL Slide-a-Lyzer cassettes as described above and performing an overnight dialysis against a 10% (w/v) solution of polyethylene glycol (PEG). The concentration of the silk solution was once again determined as described above, and the silk solution was diluted to 8% (w/v) with distilled H<sub>2</sub>O. The 8% (w/v) silk solution was stored at 4°C in Falcon tubes for future use.

### *ii) Microsphere Formation:*

Glass test tubes (16x100mm) were coated with 200mg of 1,2-Dioleoyl-*sn*-Glycero-3-Phosphocholine (DOPC) lipid powder dissolved in 0.75mL chloroform by rotating the solution while drying with low flow N<sub>2</sub> gas. Tubes were allowed to dry overnight at room temperature. Silk solution (2 mL) containing 0.1mg/mL of UN3, biotinylated-Comb1, or FITC-Comb1 was added to each glass test tube and pipetted over the walls repeatedly to hydrate the lipid film. The solution was then transferred to a Falcon tube, and the glass test tube was washed with 1mL distilled H<sub>2</sub>O, which was then also transferred to the same Falcon tube. Each 3 mL solution was then pipetted drop wise into 50 mL of distilled H<sub>2</sub>O with fast stirring. The Falcon tube was rinsed with 10 mL distilled H<sub>2</sub>O, which was also added to the stirred solution. The solution was transferred to Falcon tubes and immediately incubated at -80 °C freezer. The solutions were allowed to freeze overnight. Each peptide type of microsphere was formed in triplicate.

### *iii) Microsphere Processing:*

Tubes of frozen solution were lyophilized for three days in a Labconco 10 model lyophilizer at a pressure <110 µm of mercury and at -80 °C. Each tube of lyophilized product was dissolved in 25mL methanol, and the supernatant was transferred to a new Falcon tube to separate microspheres from undissolved silk. The tubes were centrifuged in a fixed angle rotator at 10,000rpm for five minutes at 4 °C. The supernatant was poured off and the microsphere pellet was dried overnight at room temperature. Microspheres were stored at 4 °C for future use.

## *III. ELISA Development*

### *A. Materials*

ELISA kit was obtained from Bethyl Laboratories (Montgomery, TX). Streptavidin-horseradish peroxidase conjugate and horseradish peroxidase-goat anti-rabbit IgG were obtained from Invitrogen (Carlsbad, CA). Unpurified rabbit anti-UN3 primary antibody was kindly provided by Dr. Ira Herman.

## B. Standard Curve Development

### *i) Biotinylated-Comb1 ELISA*

All buffers and solutions were prepared according to the manufacturer's instructions. Biotinylated-Comb1 was serially diluted 1:2 in coating buffer to create a total of seven dilutions ranging from 1000 ng/mL to 15.63 ng/mL, a range which was projected to encompass the release concentration from 5.0 g of biotinylated-Comb1 microspheres based on FITC-Comb1 microsphere release data. Each solution (100  $\mu$ L) was aliquotted into a clear-bottom 96-well plate, with eight replicates for each dilution. Pure coating buffer (100  $\mu$ L) was used as a 0 ng/mL control. The plate was covered and incubated on a shaker at room temperature for 60 minutes. The solution was removed from all wells, and each well was washed with 200  $\mu$ L wash solution three times. Blocking solution (200  $\mu$ L) was added to each well, and the plate was covered and incubated on a shaker at room temperature for 30 minutes. The blocking solution was then removed from all wells and each well was again washed with 200  $\mu$ L wash solution three times. Streptavidin-horseradish peroxidase conjugate was diluted to 1  $\mu$ g/mL and 0.5  $\mu$ g/mL in conjugate diluent. Each solution (100  $\mu$ L) was transferred to half of the wells, with four serial dilutions per condition. The plate was covered and incubated on a shaker at room temperature for 60 minutes. The solution was removed from all wells and each well was washed with 200  $\mu$ L wash solution five times. Fresh substrate solution was prepared according to the manufacturer's instructions and 100  $\mu$ L were added to each well within fifteen minutes of preparation. The plate was incubated at room temperature for five minutes, and the reaction was stopped with 1M H<sub>2</sub>SO<sub>4</sub> in each well. The absorbance of each well

was then read at 450nm using SOFTmax PRO 4.3 LS software and a VERSAmax Tunable Microplate Reader (Molecular Devices) within 30 minutes of plate development.

*ii) UN3 ELISA*

All buffers and solutions were prepared according the manufacturer's instructions. UN3 was serially diluted 1:2 in coating buffer to create a total of seven dilutions (see Table 1), a range which was projected to encompass the release concentration from 5.0 g of UN3 microspheres, based on FITC-Comb1 microsphere release data. 100  $\mu$ L of each solution was aliquotted into a clear-bottom 96-well plate, with 16 replicates for each dilution. 100  $\mu$ L of pure coating buffer was used as a 0 ng/mL control. The plate was covered and incubated on a shaker at room temperature for 60 minutes. The solution was removed from all wells, and each well was washed with 200  $\mu$ L wash solution three times. 200  $\mu$ L of blocking solution was added to each well, and the plate was covered and incubated on a shaker at room temperature for 30 minutes. The blocking solution was then removed from all wells and each well was again washed with 200  $\mu$ L wash solution three times. Unpurified rabbit anti-UN3 primary antibody was diluted in conjugate diluent as shown in Table 1. 100  $\mu$ L of each solution was transferred to the 96-well plate, with two replicate serial dilutions per condition. The plate was covered and incubated on a shaker at room temperature for 60 minutes. The solution was removed from all wells and each well was washed with 200  $\mu$ L wash solution three times. Concentrated horseradish peroxidase-goat anti-rabbit IgG antibody was diluted in conjugate diluent as shown in Table 1. 100  $\mu$ L of each solution was transferred to the 96-well plate, with two replicate serial dilutions per condition. The plate was covered and incubated on a shaker at room temperature for 60 minutes. The solution was removed from all wells and each well was washed with 200  $\mu$ L wash solution five times. Fresh substrate solution was prepared according to manufacturer's instructions and 100  $\mu$ L were added to each well within fifteen minutes of preparation. The plate was incubated at room temperature for five minutes, and the reaction

was stopped with 1M H<sub>2</sub>SO<sub>4</sub> in each well. The absorbance of each well was then read at 450nm using SOFTmax PRO 4.3 LS software and a VERSAmax Tunable Microplate Reader (Molecular Devices) within 30 minutes of plate development.

<b>Table 1. Standard curves constructed for UN3 ELISA development</b>			
	Standard Curve Range (ng/mL)*	Primary Antibody Concentration (µg/mL)	Secondary Antibody Dilution
<b>1</b>	1000 – 15.63	0.5	1:10000
<b>2</b>	1000 – 15.63	0.5	1:3000
<b>3</b>	1000 – 15.63	1.0	1:10000
<b>4</b>	1000 – 15.63	1.0	1:3000
<b>5</b>	2000 – 31.25	5.0	1:3000
<b>6</b>	2000 – 31.25	10	1:3000
<b>7</b>	2000 – 31.25	20	1:1000
<b>8</b>	2000 – 31.25	30	1:1000
<b>9</b>	2000 – 31.25	50	1:500
<b>10</b>	2000 – 31.25	100	1:500
<b>11</b>	2000 – 31.25	200	1:500

\*Each standard curve was constructed from seven 1:2 serial dilutions as well as a 0 ng/mL control

#### IV. Release Studies

##### A. Materials

DPBS was purchased from Invitrogen (Carlsbad, CA). Hexafluoroisopropanol was obtained from Sigma-Aldrich (St. Louis, MO). Low-bind 1.5 mL tubes were purchased from Eppendorf (Hauppauge, NY).

##### B. Fourteen-day Release Studies

###### i) FITC-Comb1

Microspheres (5.0mg) were added to 1 mL of 1x DPBS in a low-bind Eppendorf tube, broken up manually via pipet tip to promote good dispersion within the solution, and incubated at 37°C. The microsphere solutions were removed from the incubator at 24 hours and 3, 6, 10 and 14 days after the start of incubation, mixed briefly and then centrifuged in an Eppendorf 5417R centrifuge at 10,000 rpm

and 4 °C for 5 minutes. The supernatant was then pipetted into low-bind Eppendorf tubes and stored at -20 °C, whereas the microsphere-containing pellet was resuspended in 1 mL 1x DPBS and replaced in the 37 °C incubator until the next time point. The supernatant was later thawed and quantified by aliquoting 100 µL of solution into a clear-bottom 96-well plate, with two replicates for each sample. The fluorescence was then read at an excitation wavelength of 495 nm and an absorption wavelength of 525 nm using SOFTmax PRO 4.3 LS software and a VERSAmax Tunable Microplate Reader (Molecular Devices).

#### *ii) Biotinylated-Comb1 and UN3*

The study was performed as described above, with the following modifications: 10.0 mg of UN3 and biotinylated-Comb1 was used rather than 5.0 mg, and additional time points were done at two and three days in addition to one, four, six, ten and fourteen days. The released peptides were assayed by ELISA, as described above.

#### *iii) Peptide Loss and Total Peptide Content Quantification*

Undissolved silk and methanol obtained during FITC-Comb1 microsphere formation were allowed to dry at ambient conditions overnight. Known masses of dried undissolved silk as well as each type of microsphere (all near 1 mg) were added to capped glass tubes and dissolved in 1 mL of hexafluoroisopropanol (HFIP) overnight at ambient conditions to dissociate the peptides from the silk fibroin. The solutions were then uncapped and allowed to dry overnight at ambient conditions. The contents of each glass tube, as well as the dried methanol residue, were each resuspended in 1 mL 1x DPBS and stored at -20 °C. These solutions were later thawed and their peptide content quantified via a fluorescence assay.

### C. Quantification of Peptide

ELISA was conducted as described above in “biotinylated-Comb1 ELISA”. All wells were run in triplicate. For biotinylated-Comb1, streptavidin-horseradish peroxidase conjugate was used at a dilution of 0.5 µg/mL. For UN3, the primary antibody was used at a concentration of 50 µg/mL, and the secondary antibody was diluted 1:500. For FITC-Comb1, a fluorescence assay was used instead.

## *V. Cell Studies*

### *A. Materials*

Growth factor-reduced (GFR) Matrigel was obtained from BD Sciences (Bedford, MA; Cat. #354230). Bovine retinal endothelial cells (BREC) were kindly donated by Dr. Ira Herman. Eight-well chamber slides were obtained from BD Sciences. Transwell plates (24-well, pore size: 0.4 µm) were obtained from Corning Incorporated (Corning, NY).

### *B. Tube Proliferation Studies*

#### *i) Tube Proliferation Study in Eight-Well Chamber Slides*

GFR Matrigel was thawed at 4 °C overnight and 300 µL was plated on to the eight-well chamber slides at 4 °C to avoid premature polymerization. Matrigel was then polymerized at 37 °C for one hour. Post-17<sup>th</sup> passage BRECs were plated onto the polymerized Matrigel at a concentration of  $5 \times 10^4$  cells/well. Negative control cells were plated in 200 µL DMEM containing 1% BCS. Stock solutions of positive controls were prepared in Tris (pH 8.0) and added to the cells in 1% DMEM at a concentration of 10 ng/mL bFGF, 100 nM Comb1, 25 nM UN3, and 100 nM Comb1 and 25 nM UN3 together. Solutions of FITC-Comb1, biotinylated-Comb1, UN3 and MilliQ obtained after the first day of the release profile study were thawed and diluted in DPBS to match control concentrations, and then 100 µL of each solution in 100 µL of DMEM with 2% BCS was added to the cells. Solutions of FITC-Comb1, biotinylated-Comb1, UN3 and MilliQ microspheres (100 µL) were also prepared so that the projected 24-hour release

of each solution would equal the control concentration (based on FITC-Comb1 release profile studies), and added to the cells as described above. Each condition was performed in duplicate. Cells were placed back in 37 °C and imaged at six and 24 hours post-plating. Visualization of endothelial sprout formation was performed with an Axiovert 200M microscope (Carl Zeiss MicroImaging, Thornwood, NY) using a 10x objective lens. Image analysis and tube lengths were measured using ImageJ (NIH).

*ii) Tube Proliferation Study in 24-Well Transwell Plate*

The tube proliferation study was redesigned by the author and repeated in a transwell plate to accommodate for an observed tendency of the microspheres to aggregate on the surface of BRECs, thus inhibiting imaging of the cells. By adding the microspheres to transwells rather than directly to the cells and then removing the transwells during imaging, it was possible to expose the BRECs to the breakdown products of the microspheres without allowing them to obscure the cells. GFR Matrigel was thawed at 4 °C overnight and then plated on to the 24-well chamber slides in a thin layer by adding 300 µL per well, spreading it around evenly and then pipetting off the excess at 4 °C to avoid premature polymerization. Matrigel was then polymerized at 37 °C for 30 minutes. Post-13<sup>th</sup> passage BREC were plated onto the polymerized Matrigel at a concentration of 5x10<sup>4</sup> cells/well in 600 µL DMEM with 1% BCS. Stock solutions of positive controls were prepared in Tris (pH 8.0) and 150 µL was added to the transwells for a final concentration of 10 ng/mL bFGF, 100 nM Comb1, and 125 nM UN3. Stock solutions of FITC-Comb1, biotinylated-Comb1, UN3 and MilliQ obtained after the first day of the release profile study as well as FITC-Comb1, biotinylated-Comb1, UN3 and MilliQ microspheres were prepared in 1x DPBS and added to the transwells as above for a final concentration matching that of the controls. Each condition was performed in duplicate. Cells were placed back in 37 °C and imaged at five and 24 hours post-plating. Visualization of endothelial sprout formation was performed with an Axiovert 200M microscope (Carl

Zeiss MicroImaging, Thornwood, NY) using a 5x objective lens. Image analysis and tube lengths were measured using ImageJ (NIH).

#### *VI. Statistical Analysis*

Counts obtained in the tube proliferation study were recorded manually and analyzed using Microsoft Excel (Microsoft, Redmond, WA). Results are presented as mean $\pm$ SEM. Statistical significance was determined using a two-tailed heteroscedastic t-test. A value of  $p < 0.05$  was considered a significant deviation from the control.

## Results

### I. Release Profile Study

Preliminary studies measured the release of FITC-Comb1, biotinylated-Comb1 and UN3 from 8% silk microspheres to establish a characteristic release profile for each. For the FITC-Comb1 microspheres, plates were read using an excitation wavelength of 495nm and an emission wavelength of 525nm. For the biotinylated-Comb1 and UN3 microspheres, absorbance of the horse radish peroxidase substrate was measured at 450nm. A standard curve was constructed in each case using the respective peptides dissolved in DPBS. Data was also obtained from control microspheres to account for fluorescence or absorbance generated by the silk fibroin itself. This data was subtracted from the microsphere data for

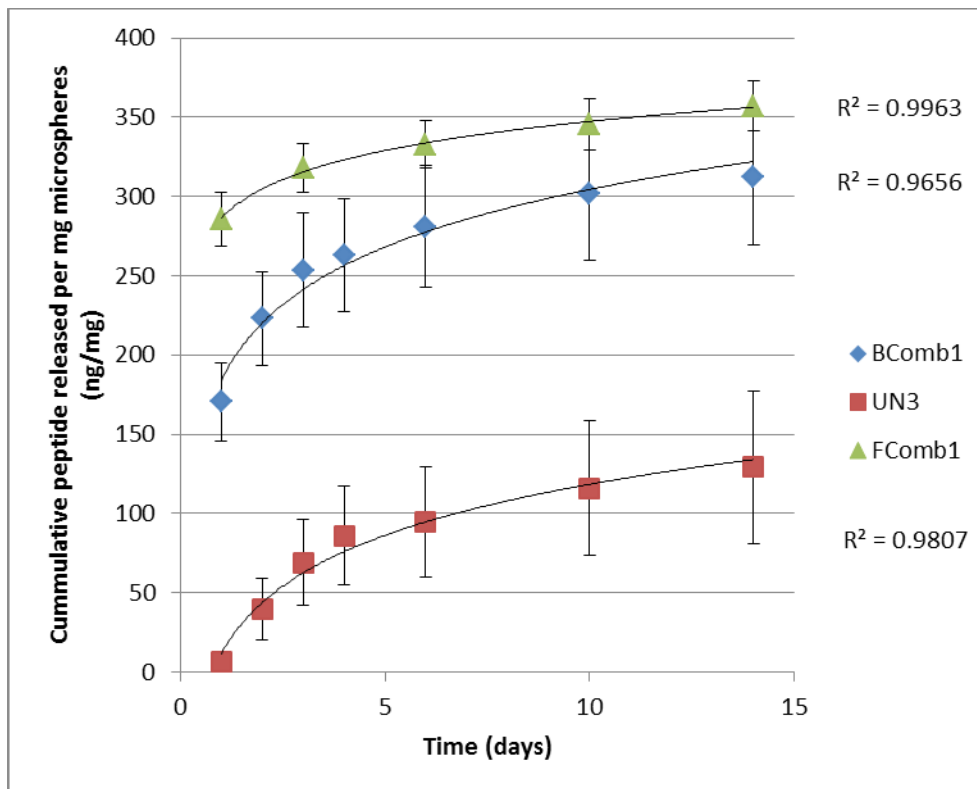


**Figure 1.** Cumulative mass release (ng) of biotinylated-Comb1 (BComb1), FITC-Comb1 (FComb1) and UN3 per 1 mg of microspheres as measured by ELISA and a fluorescence assay. Error bars represent SEM.

each day.

As demonstrated in Figure 1, the bulk of the total release for Comb1-containing microspheres occurred within twenty-four hours, with an average of 285.4 ng/mg microspheres for FITC-Comb1 and 170.4 ng/mg microspheres for biotinylated-Comb1. Release slowed down after this initial burst, reaching a cumulative 318.0 ng/mg for FITC-Comb1 and 253.6 ng/mg for biotinylated-Comb1 by day three. The final cumulative release after 14 days was 357 ng/mg for FITC-Comb1 and 312.5 ng/mg for biotinylated-Comb1.

For UN3-loaded microspheres, initial release was low, with only 6.4 ng/mg microspheres after 24 hours. However, release rose to a cumulative 69.0 ng/mg after three days, and the final 14-day cumulative release for UN3 was 129.3 ng/mg. Figure 2 shows the average cumulative release profile of the FITC-Comb1 microspheres. All three release profiles fit a logarithmic regression with high correlation, with  $R^2 = 0.9963$  for FITC-Comb1,  $R^2 = 0.9656$  for biotinylated-Comb1, and  $R^2 = 0.9807$  for UN3, which is the desirable outcome because it make release at other time points easy to predict, and

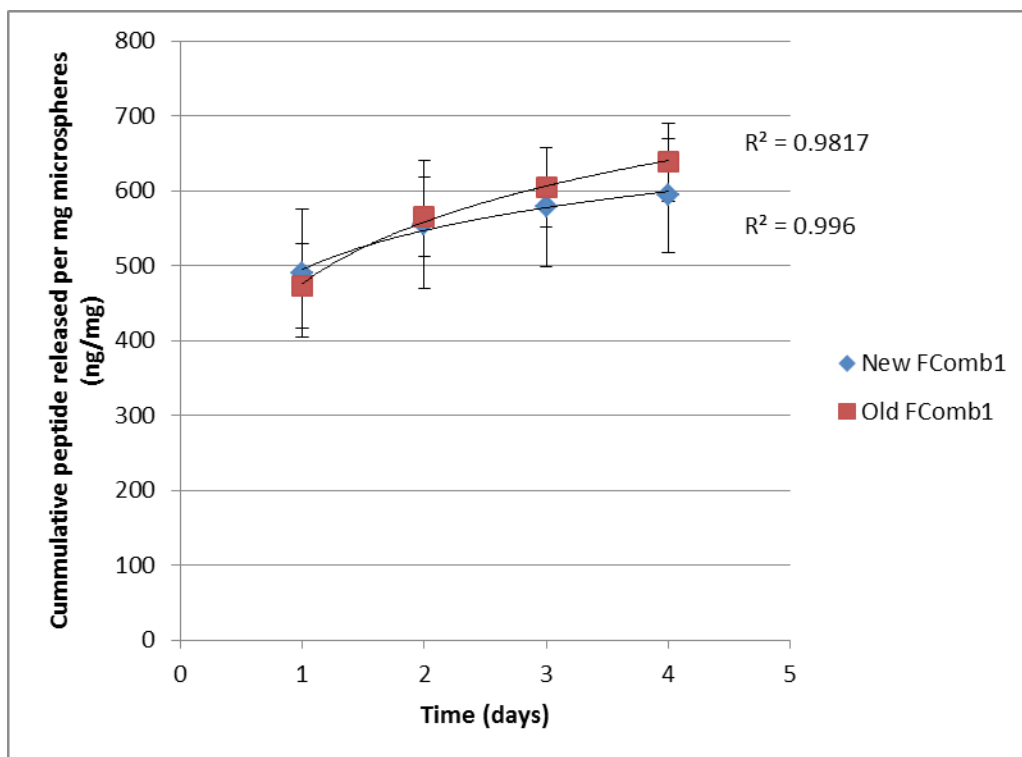


**Figure 2.** Cumulative mass release (ng) of new (<1 week old) FITC-Comb1 and old (7.5 months) FITC-Comb1 from 1mg microspheres. Concentrations obtained via a fluorescence assay. Error bars represent SEM.

makes it easy to determine how much of a given microsphere should be administered for a desired amount delivered.

In addition, microspheres that had been stored at 4°C for 7.5 months were assayed for four days to determine whether prolonged storage had any effect on the release of or ability to detect the peptides. As shown in Figure 2, old FITC-Comb1 microspheres showed no statistically significant difference in release from new FITC-Comb1 microspheres. Furthermore, both release profiles fit logarithmic regression curves with high correlation, at  $R^2 = 0.996$  for the new FITC-Comb1 microspheres and  $R^2 = 0.9817$  for the old FITC-Comb1 microspheres.

However, biotinylated-Comb1 microspheres showed an entirely different trend (Figure 3). The new microspheres displayed a logarithmic release profile ( $R^2 = 0.9875$ ), whereas the old microspheres displayed a linear ( $R^2 = 0.9778$ ), near-zero release. Only one replicate of old biotinylated-Comb1 spheres

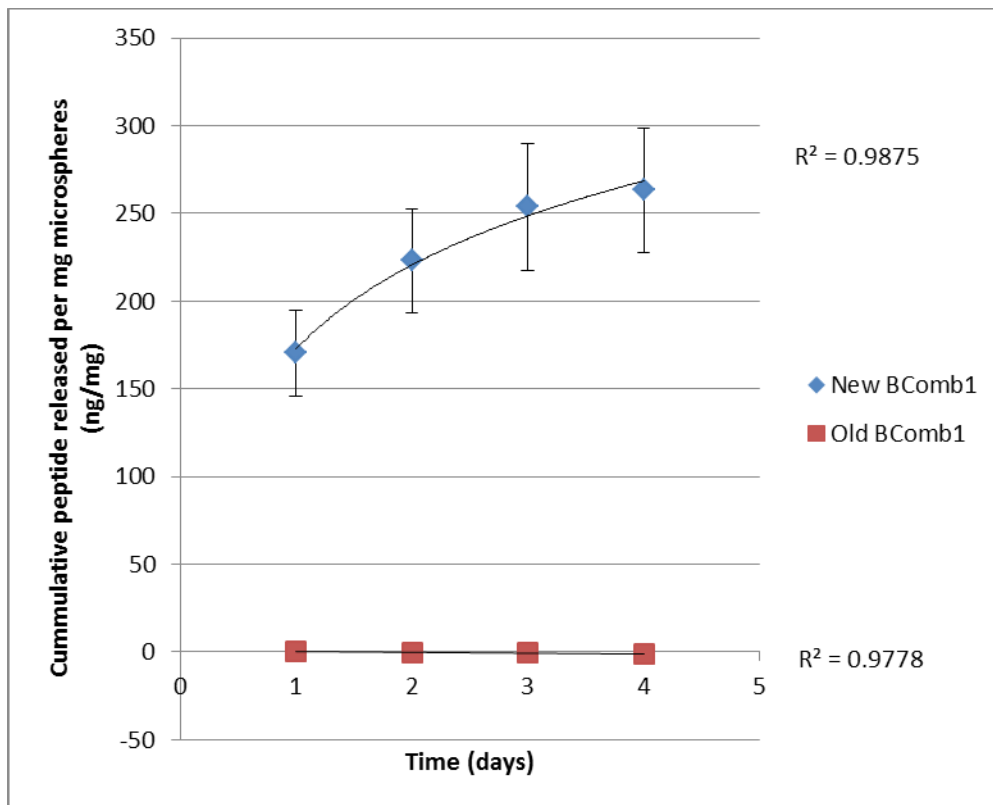


**Figure 3.** Cumulative mass release (ng) of new (<1 week old) biotinylated-Comb1 and old (7.5 months) biotinylated-Comb1 from 1mg microspheres. Concentrations obtained via an ELISA. Error bars represent SEM.

was available, and thus statistical analysis could not be performed comparing the two curves. However, considering that the same loading and microsphere formation protocol was used for both sets of microspheres, it is clear that the two release profiles are quite different.

Finally, for UN3-loaded microspheres (Figure 4), the release profiles of both the new and the old microspheres followed logarithmic release curves with  $R^2 = 0.9916$  and  $R^2 = 0.9897$ , respectively.

Although the mean cumulative release was lower for the old UN3 than the new UN3 microspheres, no

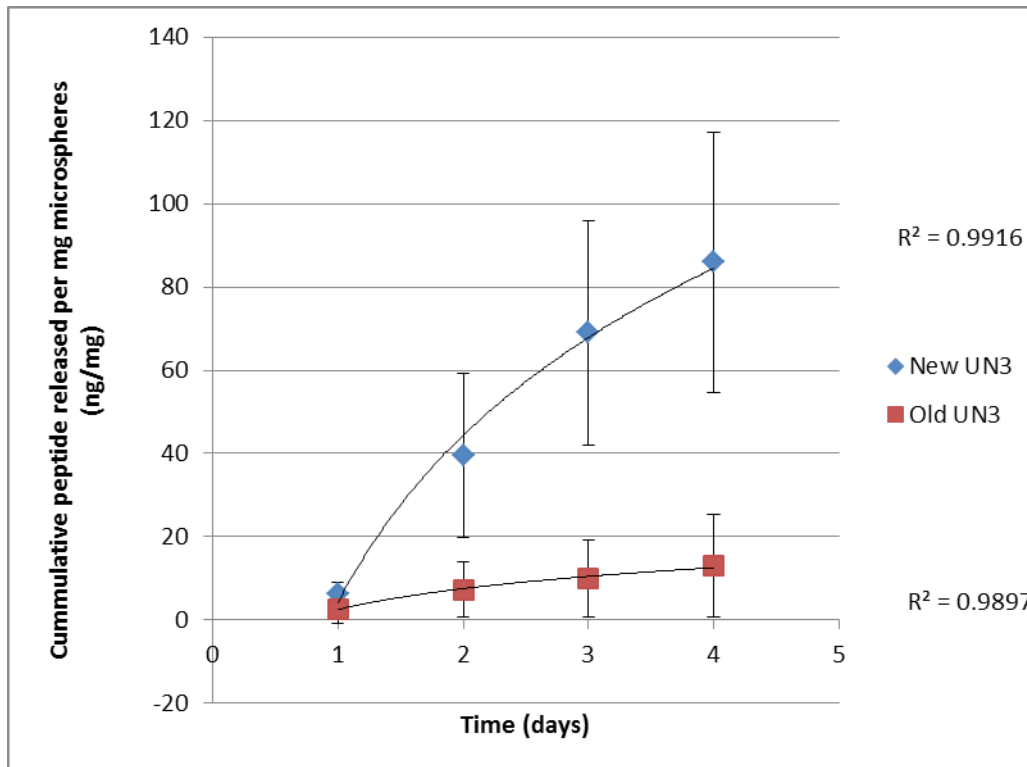


**Figure 4.** Cumulative mass release (ng) of new (<1 week old) UN3 and old (7.5 months) UN3 from 1mg microspheres. Concentrations obtained via ELISA. Error bars represent SEM.

statistically significant difference between the two curves was found. These findings indicate that

whereas FITC-Comb1 release from silk microspheres does not change with prolonged storage and the FITC tag itself is not degraded by it, the biotin tag is clearly affected by storage and is either degraded or binds to the silk, preventing release of the peptide. Finally, UN3 must undergo a conformational change while in storage which accounts for the loss of the epitope used to detect it in an ELISA assay.

## II. Protein Loss

In order to be able to encapsulate peptides in silk microspheres with a specific target level of peptide release, it is important to determine how much of the peptide that is being added to the microspheres in the beginning of the process is actually released in the end. Table 2 shows the

**Table 2. Cumulative percent of initially added peptide that is released (%). All values given as mean±SEM.**

After 24 Hours			After 3 Days			After 14 Days		
<i>FComb1</i>	<i>BComb1</i>	<i>UN3</i>	<i>FComb1</i>	<i>BComb1</i>	<i>UN3</i>	<i>FComb1</i>	<i>BComb1</i>	<i>UN3</i>
8.90±0.16	7.11±0.55	0.18±0.07	10.33±0.68	9.80±1.59	1.99±0.69	22.00±0.20	12.14±2.05	3.73±1.23

cumulative percentage of the amount of each peptide initially added to the microspheres that is released by a certain time point. Whereas FITC-Comb1 appears to have the best release statistics, exceeding 10% of initial load released by day 3 and reaching 22% after 14 days, UN3 does not appear to release well from the microspheres, totaling a mere 2% after 3 days and 3.7% at the end of the 14 day trial. It is interesting to note that biotinylated-Comb1 lags behind FITC-Comb1 in release from the microspheres, even though they nearly identical peptides differing only by the functional tag (FITC or biotin). This analysis determined the relative efficiencies of using silk microspheres as a drug delivery system for the three peptides. Although the system works relatively well for Comb1 derivatives, it appears that UN3 is either not effectively incorporated into or released from silk microspheres.

In addition, a pilot study was run with FITC-Comb1 to determine when peptide loss occurred during the microsphere formation process. Both the FITC-Comb1 silk microspheres and the silk residue remaining from microsphere formation were dissolved in HFIP, and the freed peptide was resuspended in DPBS and assayed by fluorescence analysis. Peptide remaining from dried methanol was similarly resuspended and assayed. Table 3 shows the percentage of FITC-Comb1 that was successfully loaded into the microspheres, as well as the percentage that was lost in the silk residue and in the methanol treatment. It should be noted that these percentages do not add up to 100%, and that there are no other intermediate steps where the peptide could have been lost, suggesting that some of the peptide, or at least its fluorescent tag, was degraded during the process of microsphere preparation.

**Table 3. Distribution of initial FITC-Comb1 during microsphere formation and processing. All values are given as mean±SEM.**

Total Loading	Loss in Silk	Loss in Methanol
9.79±0.88	26.19±17.74	1.42±0.89

Furthermore, the total loading percentage for the FITC-Comb1 microspheres is 9.79±0.88%, which is less than 3-day and 14-day cumulative release percentages obtained for FITC-Comb1 microspheres (Table 2). This suggests that some of the FITC-Comb1 peptide was degraded by the HFIP treatment of the microspheres, giving a falsely low total loading value. These findings suggest that a different solvent should be tried for determining total loading, which would still dissolve silk but would not damage the peptide.

### III. ELISA Optimization Study

In order to establish a protocol for the quantification of biotinylated-Comb1 and UN3 in solution, a number of standard curves of both peptides were 2:1 diluted in DPBS and assayed with varying concentrations of primary, and in the case of UN3, secondary substrate. Figure 5 shows the

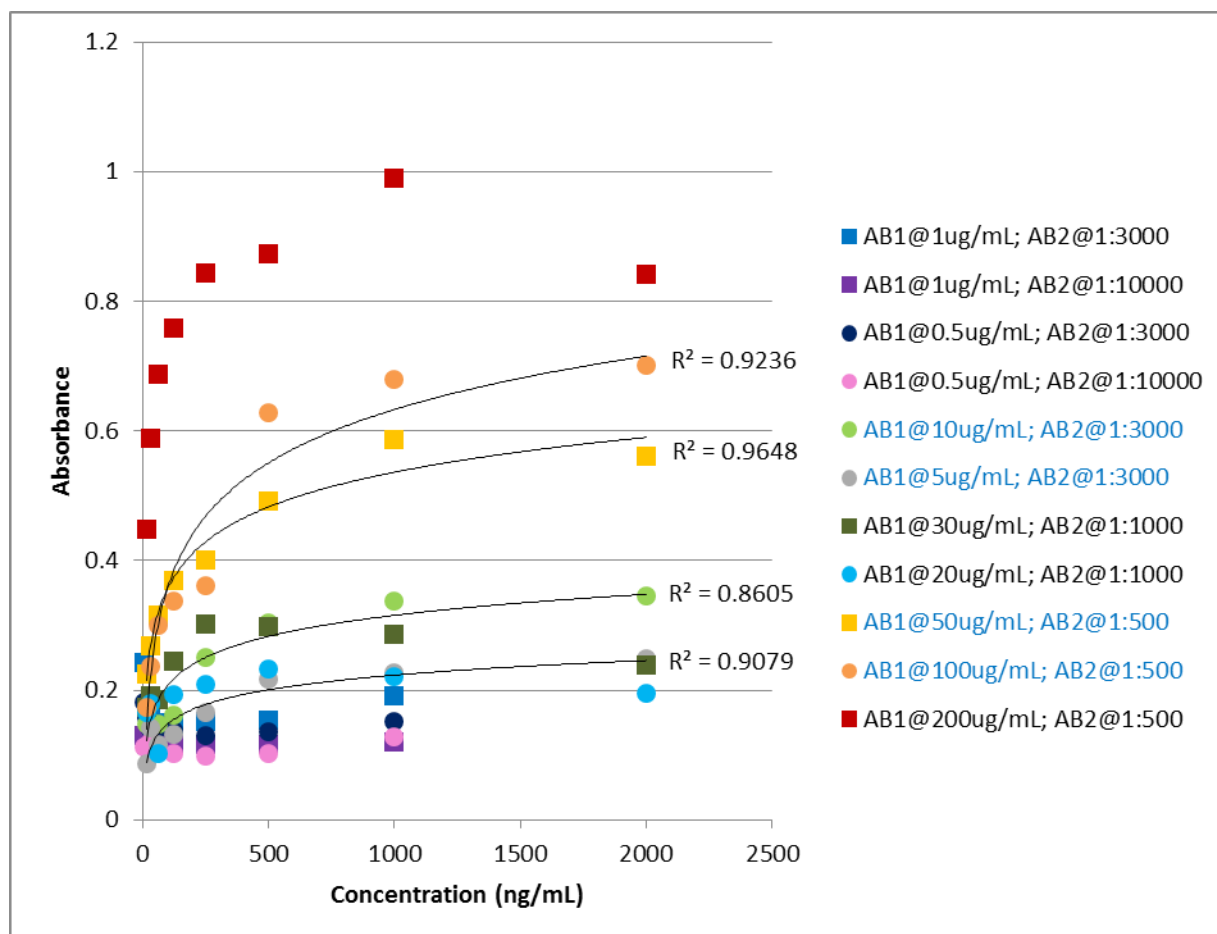


**Figure 6.** Standard curves of UN3 diluted in DPBS obtained by ELISA using varying primary (AB1) and secondary (AB2) concentrations. Regression curves are shown for correlations with an  $R^2 > 0.85$ . These standard curves are also highlighted in blue in the legend.

standard curves that were established for biotinylated-Comb1. Both standard curves created using 1  $\mu\text{g}/\text{mL}$  and 0.5  $\mu\text{g}/\text{mL}$  fit linear regression curves with high correlation, but the 0.5  $\mu\text{g}/\text{mL}$  had a higher correlation coefficient ( $R^2 = 0.9889$ , compared to  $R^2 = 0.9694$  for the 1  $\mu\text{g}/\text{mL}$  curve).

For UN3, a number of standard curves were developed in DPBS to establish one that would fit a linear, logarithmic or exponential regression curve with high correlation. Figure 6 shows all of the curves that were generated. Four standard curves fit a regression curve with an  $R^2 > 0.85$ . All of these curves fit logarithmic regressions well, however the best was the curve with the highest correlation coefficient of  $R^2 = 0.9648$ , which was generated using a primary antibody concentration of 50  $\mu\text{g}/\text{mL}$  and a secondary antibody dilution of 1:500. These concentrations were subsequently used to run further ELISAs.

#### IV. Tube Proliferation Assay

In order to establish whether peptides released from silk microspheres retained their bioactivity, the effect of the microspheres and their release solutions on tube formation in BRECs was examined through a Matrigel-based assay, which enables a quantitative analysis of endothelial morphogenesis. Previous publications (Kleinman and Martin, 2005) indicated that BRECs plated on Matrigel form lumen-

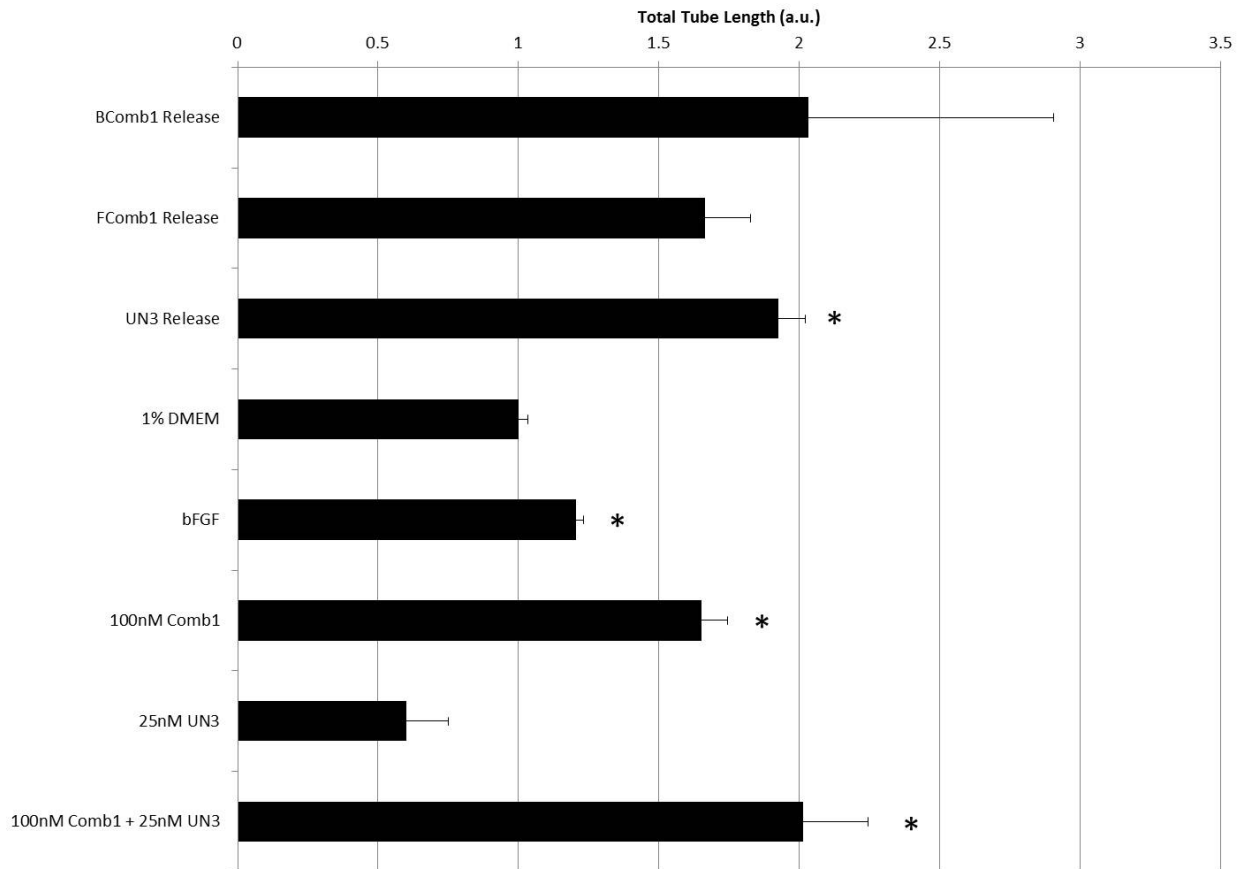


**Figure 7.** Quantitative evaluation of tube proliferation. Endothelial sprouts were images and measured manually in ImageJ at 6 hours post-plating. Two fields were evaluated for each well, with two wells per condition. Data was plotted as relative tube length compared to 1% DMEM control. Error bars represent SEM; \* $p < 0.05$  compared with control.

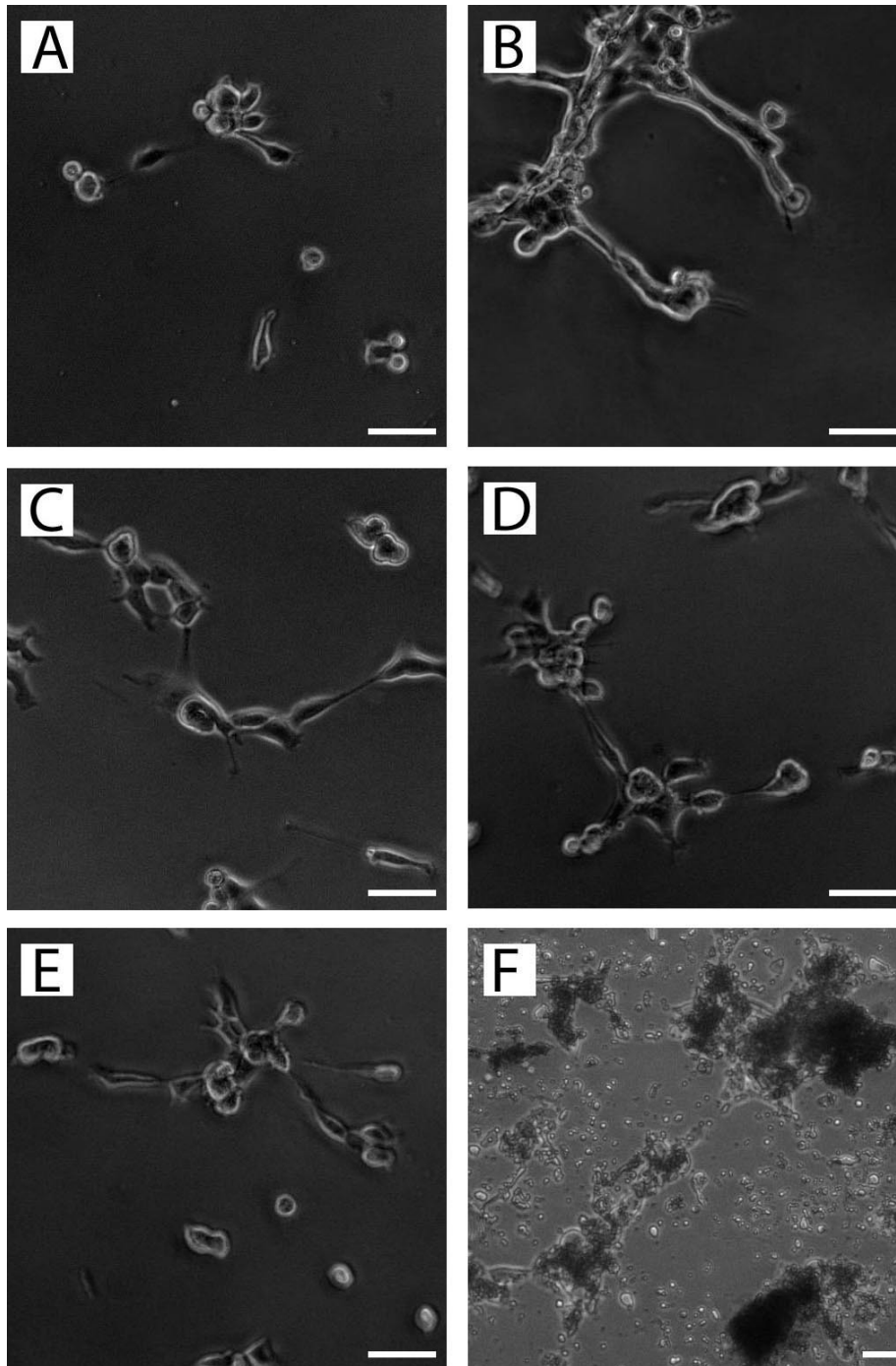


**Figure 8.** Photomicrographs of capillary-like structures formed by capillary endothelial cells cultured on Matrigel for 6 hours in (A) DMEM with 1% BCS only; (B) 10 ng/mL bFGF; (C) 100 nM Comb1; (D) 100 nM Comb1 and 25 nM UN3; (E) 25 nM UN3 microsphere release solution and (F) UN3 microspheres. (B) – (E) represent populations that showed statistically different proliferation from (A), the DMEM control, as shown in Figure 7. (F) shows silk microsphere aggregation on the surface of BREC after 6 hours incubation with UN3 microspheres. Scale bar 100  $\mu$ m.

containing structures within 6-12 hours. Therefore, morphogenesis of the BRECs was examined at 6 and 23 hours post-plating with phase-contrast microscopy. Figure 7 shows a quantitative evaluation of tube proliferation six hours post-plating. The effect of the microspheres on tube proliferation could not be recorded due to microsphere aggregation on the surface of the cells. However, it was found that the

UN3 release solution produced a 90% increase in tube proliferation as compared to the control, a difference that was found to have a statistically significant p-value. Of the positive controls, 10 ng/mL bFGF produced a 20% increase, 100 nM Comb1 produced a 65% increase, and 100 nM Comb1 combined with 25 nM UN3 produced a two-fold increase in tube proliferation, all of which were found to have statistically significant p-values. Although the other experimental groups showed variation from the control, it was not found to be statistically significant. Figure 8 shows photomicrograph images of the control cells (A) as well as treatments that showed statistical deviations from the control (B) – (E). Image (F) in Figure 8 shows the aggregation of UN3 microspheres on the surface of BRECs. It is possible that this aggregation was caused by the incomplete release of peptide from the microspheres and its subsequent binding to receptors on the cells, creating a “bridge” between the two and thus aggregating the microspheres on the cell surface. This prevented proper imaging and quantification of tube proliferation in these samples. Although the large black clumps in image F could be interpreted as dead cells, this is not supported by the endothelial sprouts that can be seen around their edges.

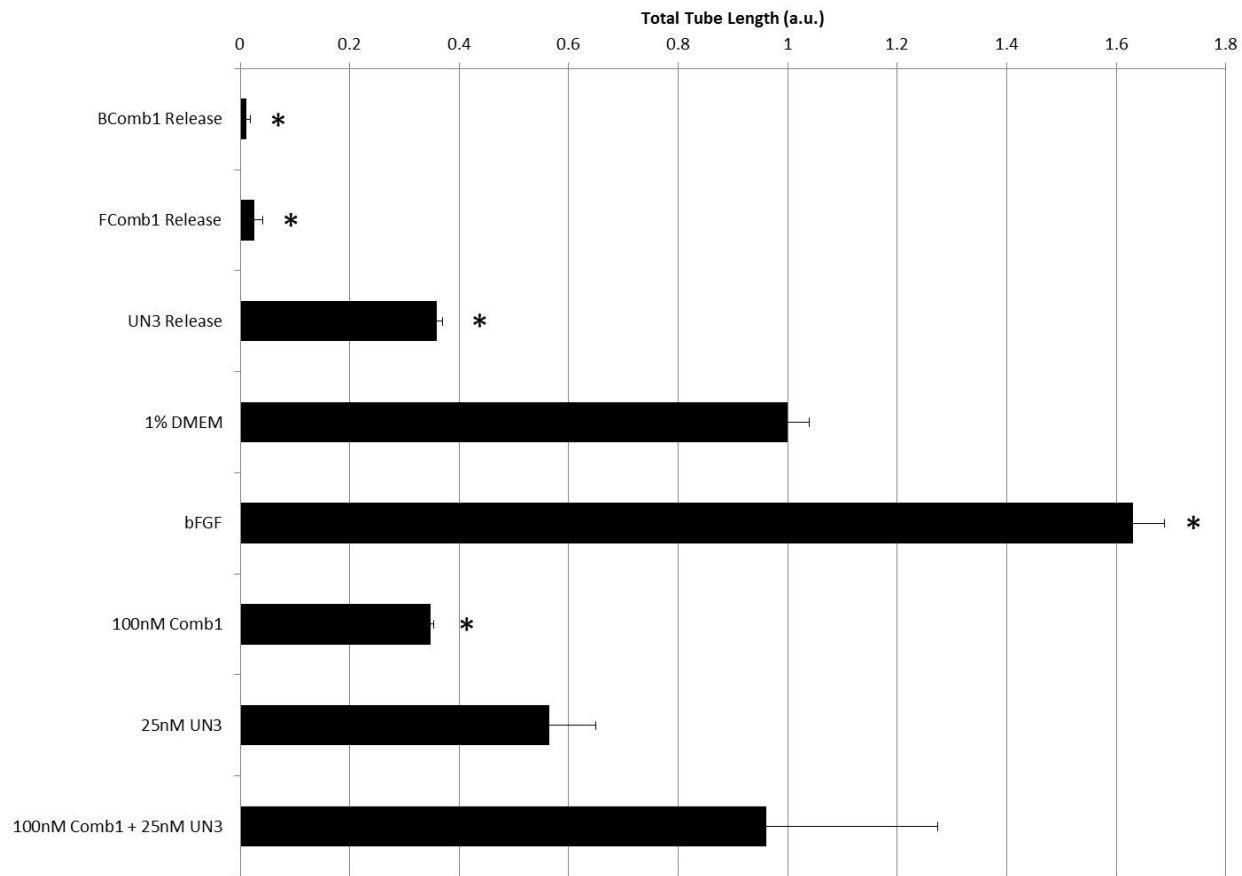


**Figure 9.** Quantitative evaluation of tube proliferation. Endothelial sprouts were images and measured manually in ImageJ at 23 hours post-plating. Two fields were evaluated for each well, with two wells per condition. Data was plotted as relative tube length compared to 1% DMEM control. Error bars represent SEM; \*p < 0.05 compared with control.

The same type of quantitative evaluation of tube proliferation was carried out 23 hours post-plating. The effect of the microspheres was once again not included due to imaging difficulties. Figure 9 indicates that the only plates treated with 10 ng/mL bFGF showed a statistically significant 63% increase in tube proliferation over the control. Cells treated with biotinylated-Comb1 and FITC-Comb1 release solutions showed nearly no tube formation at 23 hours, and cells treated with UN3 release solution showed a 65% decrease in tube formation compared to the control, as did cells treated with 100 nM Comb1. Figure 10 shows images of cells from populations that were found to differ significantly from the

control. Although the DMEM control (A) and the bFGF positive control (B) show extensive endothelial morphogenesis, the 100 nM Comb1 positive control (C) shows reduced tube proliferation, as does the

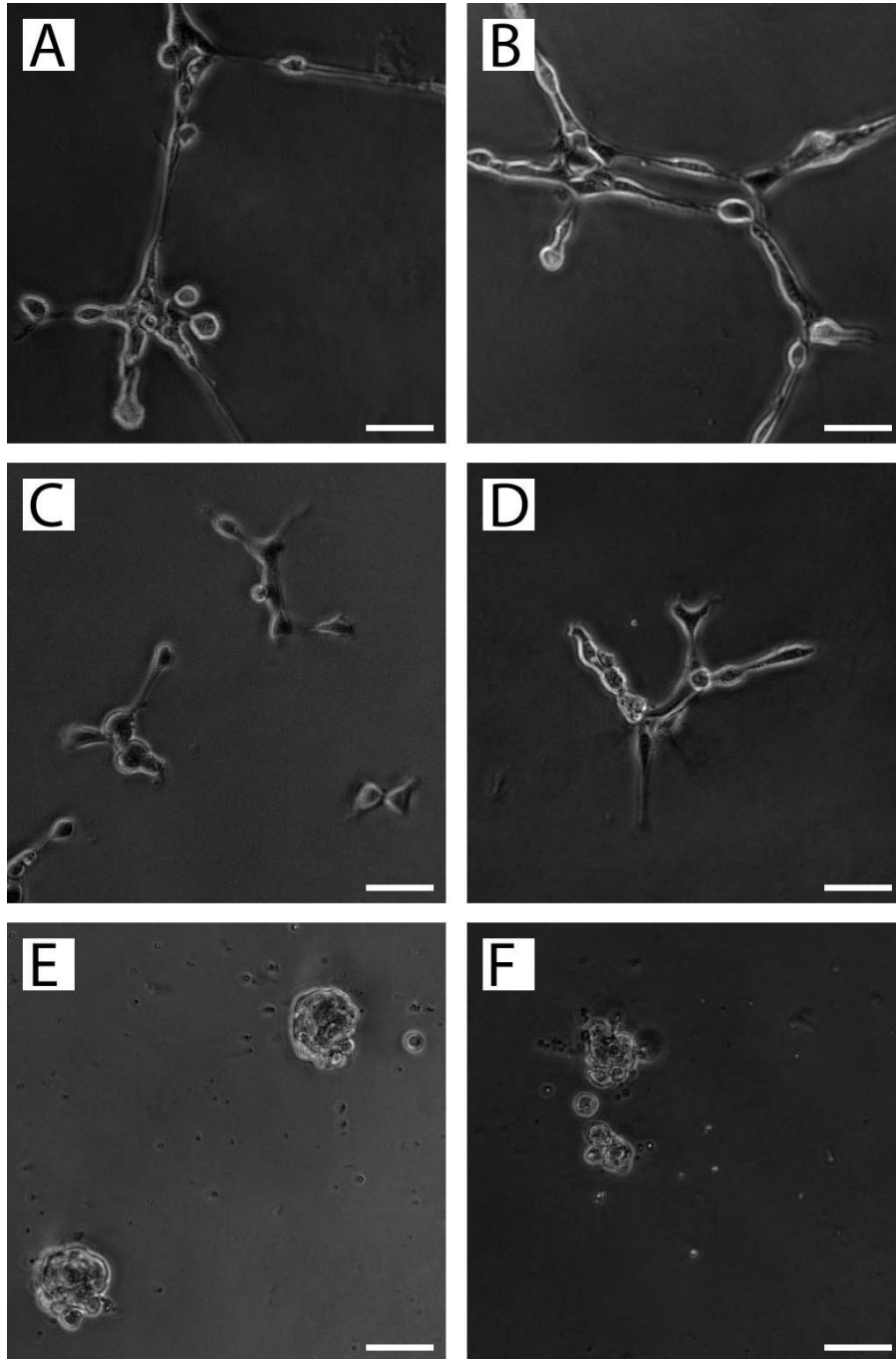


**Figure 10.** Photomicrographs of capillary-like structures formed by capillary endothelial cells cultured on Matrigel for 6 hours in (A) DMEM with 1% BCS only; (B) 10 ng/mL bFGF; (C) 100 nM Comb1; (D) 25 nM UN3 microsphere release solution; (E) 100 nM biotinylated-Comb1 microsphere release solution and (F) 100 nM FITC-Comb1 microsphere release solution. (B) – (F) represent populations that showed statistically different proliferation from (A), the DMEM control, as shown in Figure 9. Scale bar 100  $\mu$ m.

UN3 microsphere release solution (D). Cells treated with biotinylated-Comb1 and FITC-Comb1 microsphere release solution showed nearly no tube formation and appeared as isolated aggregates on

the photomicrographs. This kind of agglutination is sometimes, but not always, associated with cell death. However, even if the cells are not dead it is clear that they did not undergo any tube proliferation, suggesting that peptides released into and stored in solution did not retain their bioactivity.

A second tube proliferation study was conducted in order to better examine the effects of the silk microspheres on tube proliferation, which was prevented in the first study by the aggregation of

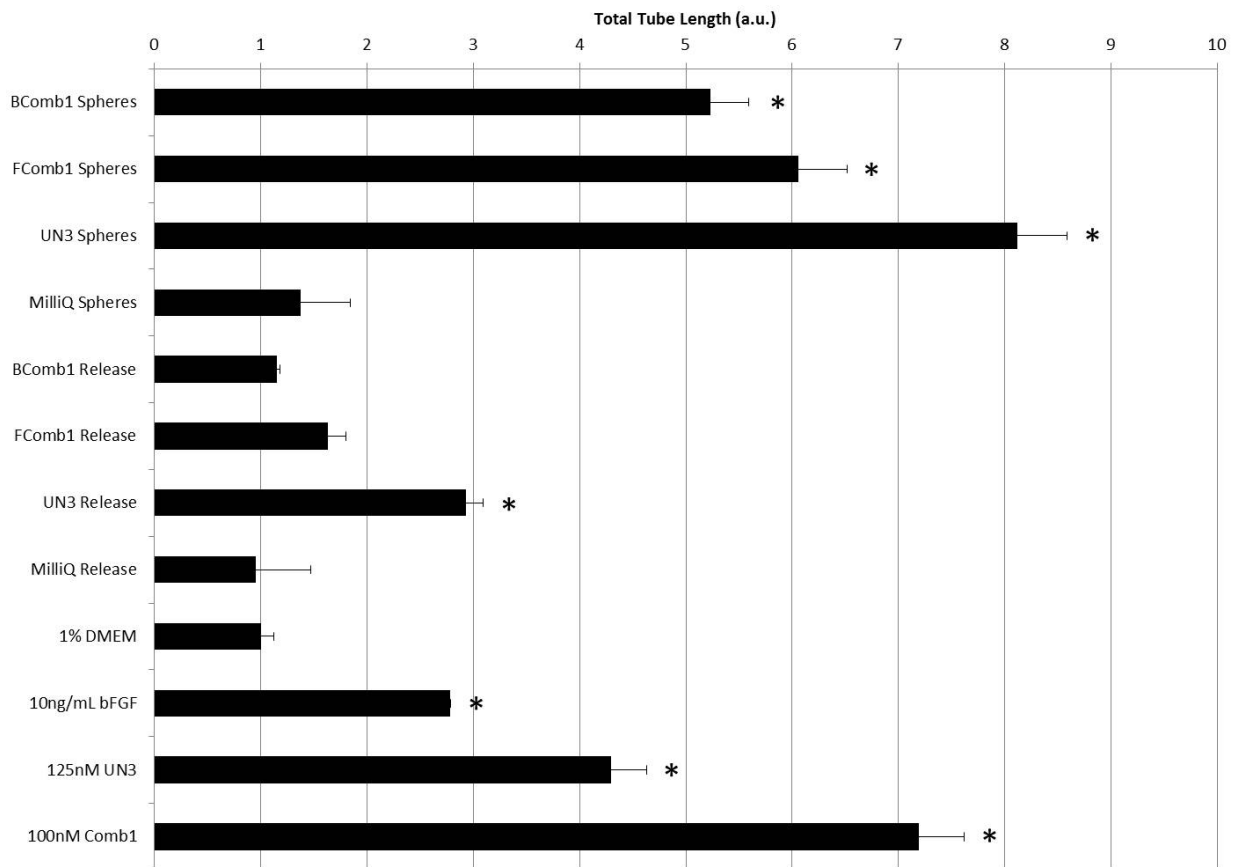


**Figure 11.** Quantitative evaluation of tube proliferation. Endothelial sprouts were images and measured manually in ImageJ at 5 hours post-plating. Two fields were evaluated for each well, with two wells per condition. Data was plotted as relative tube length compared to 1% DMEM control. Error bars represent SEM; \* $p < 0.05$  compared with control.

microspheres on the BREC surface. In this study a transwell plate was used to physically separate the microspheres from the BREC. All peptides, microspheres, and microsphere release solutions were

added to the transwells, whereas cells were plated on the bottom of each well. Transwells were perforated, which allowed passage of peptides between chambers, but the transwell pore size of 0.4  $\mu\text{m}$  did not allow the microspheres, with an average diameter of 2  $\mu\text{m}$ , to pass through (Wang *et al*, 2007).

The data indicate that at 5 hours post-plating, all three types of peptide-containing microspheres showed very high levels of endothelial morphogenesis, with biotinylated-Comb1 microspheres leading to a 5.2 fold increase, FITC-Comb1 microspheres leading to a 6.1 fold increase, and UN3 microspheres stimulating an 8.1 fold increase in tube proliferation over the DMEM control (Figure 11). The UN3 microsphere release solution also led to a significant 2.9 fold increase in endothelial morphogenesis, although the biotinylated-Comb1 and FITC-Comb1 solutions did not have a statistically significant impact on tube proliferation as compared to the control. Finally, all three positive controls showed a significant increase over the DMEM control. bFGF (10 ng/mL) caused a 2.8 fold increase in tube proliferation, 125 nM UN3 caused a 4.3 fold increase in tube proliferation, and 100 nM Comb1 caused a 7.2 fold increase. These were all much greater percentage increases than was seen in the chamber slide tube proliferation experiment. Figure 12 shows photomicrographs of the DMEM control cells (A) as well as all those cell populations that differed significantly from the control. In (E), which is the UN3 microsphere release solution treatment, the black clusters appear to be silk fragments that may have been taken up during collection of the release solution and which then diffused through the pores of the transwell. Once the effects of peptides encapsulated in silk microspheres on endothelial morphogenesis were quantifiable, they were determined to be profound. A second quantitative evaluation of tube proliferation was carried out at 23 hours post-plating. Figure 13 shows that, compared with the 5 hour time point in Figure 11, the variation among the experimental conditions was greatly reduced, with the highest levels of tube proliferation, stimulated by the FITC-Comb1 spheres, only at a 2.1 fold increase from the DMEM control. The only other significant increases from the DMEM

control are the positive controls, with a 61% increase due to 10 ng/mL bFGF and a 66% from both 125 nM UN3 and 100 nM Comb1. It appears that the tube proliferation, the extent of which varied greatly

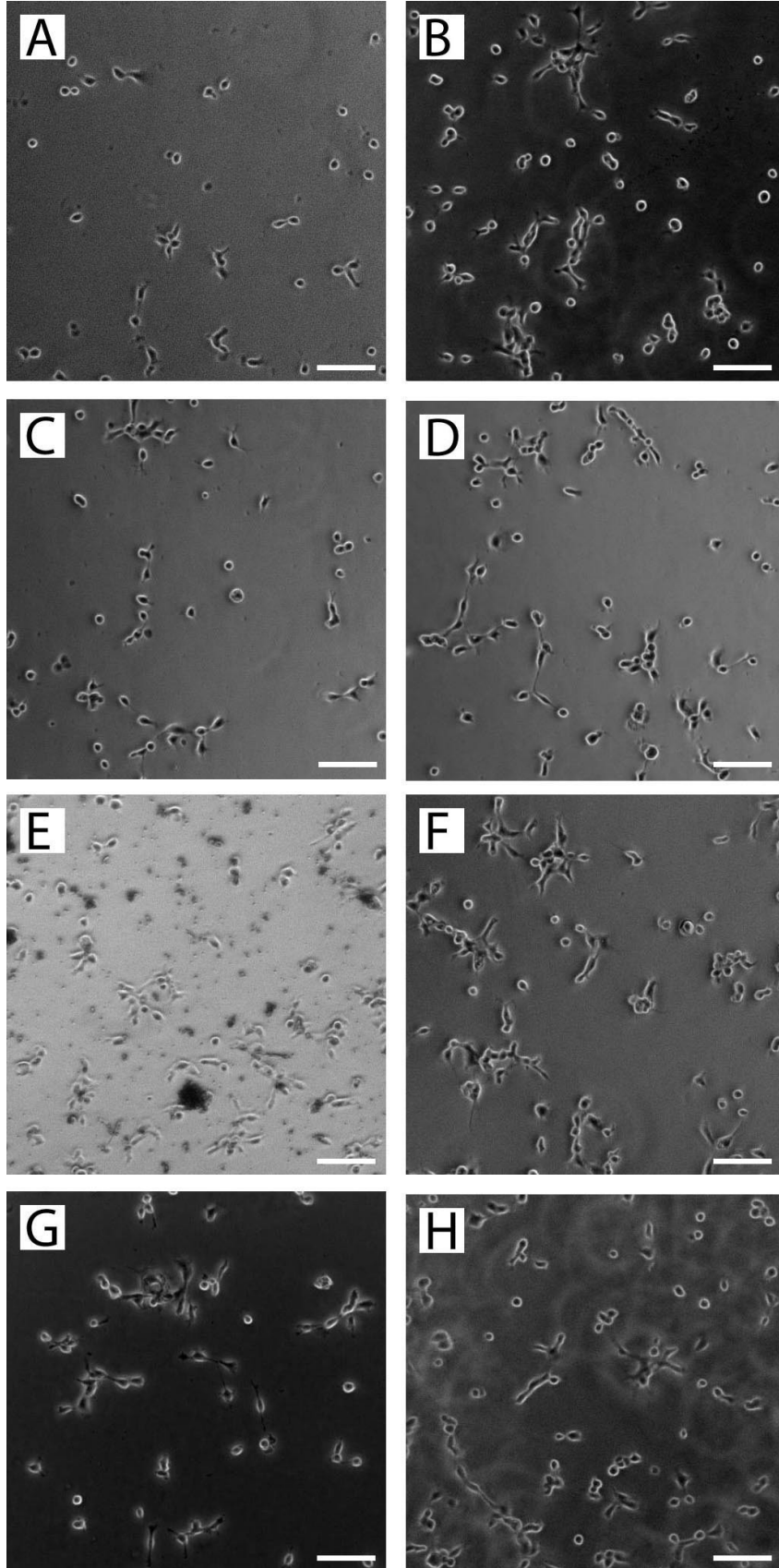


**Figure 12.** Photomicrographs of capillary-like structures formed by capillary endothelial cells cultured on Matrigel for 5 hours in (A) DMEM with 1% BCS only; (B) 10 ng/mL bFGF; (C) 125 nM UN3; (D) 100 nM Comb1; (E) 125 nM UN3 microsphere release solution; (F) UN3 microspheres; (G) biotinylated-Comb1 microspheres and (H) FITC-Comb1 microspheres. (B) – (H) represent populations that showed statistically different proliferation from (A), the DMEM control, as shown in Figure 11. (E) shows silk fragments in solution with the BRECs which were probably taken up during the collection of the UN3 microsphere release sample and later diffused through the pores in the transwell along with the peptide. Scale bar 200  $\mu$ m.

at 5 hours post-plating depending on the treatment, evened out by the 23 hour time point. The photomicrographs of the cells at 23 hours post-plating (Figure 14) show a fairly dense network of capillary-like tubes, suggesting that the tube proliferation may have reached a saturation point beyond which it either proceeds more slowly or stops altogether.

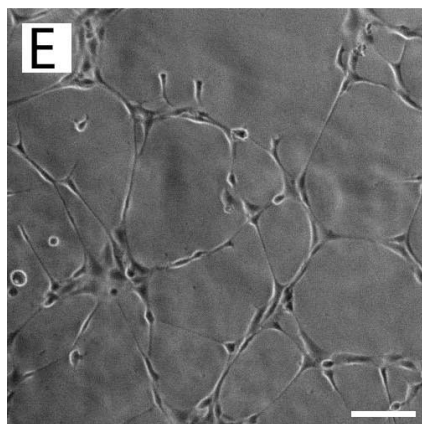
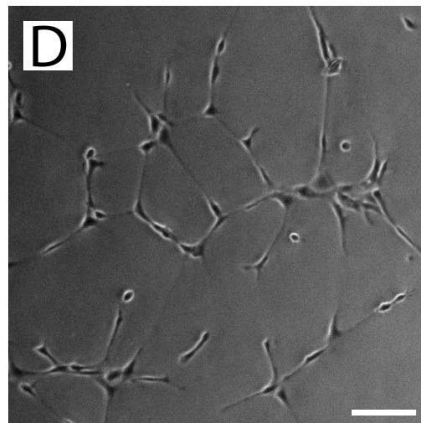
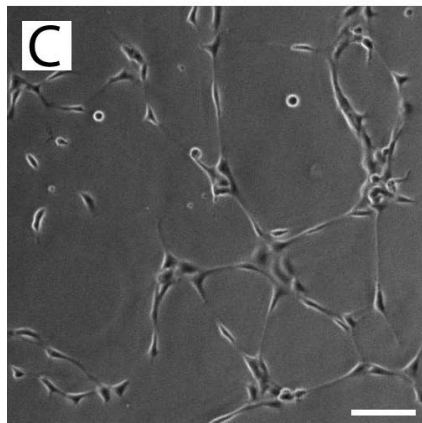
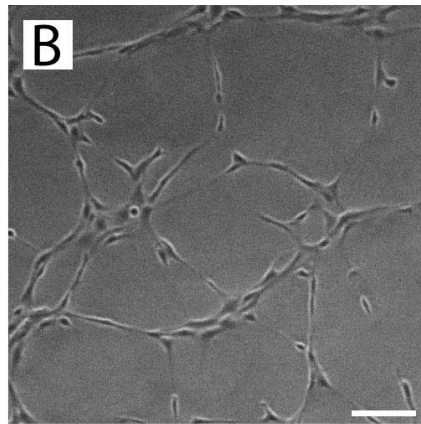
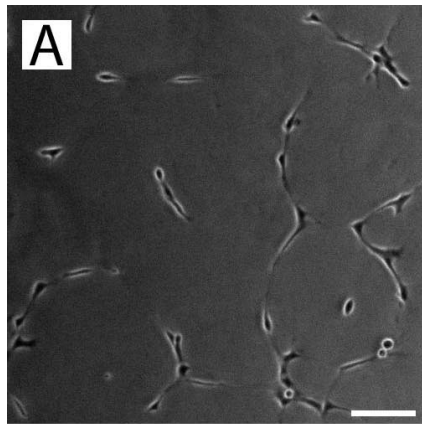


**Figure 14.** Photomicrographs of capillary-like structures formed by capillary endothelial cells cultured on Matrigel for 23 hours in (A) DMEM with 1% BCS only; (B) 10 ng/mL bFGF; (C) 125 nM UN3; (D) 100 nM Comb1 and (E) FITC-Comb1 microspheres. (B) – (E) represent populations that showed statistically different proliferation from (A), the DMEM control, as shown in Figure 13. Scale bar 200  $\mu$ m.

\*  
\*  
\*

outs were images and measured for each well, with two wells per EM control. Error bars represent



## Discussion

Preliminary studies established well-defined release profiles for UN3, biotinylated-Comb1, and FITC-Comb1 from silk microspheres. These release profiles, recorded over a two week period, all fit logarithmic regression curves with high correlation. Generating these curves enables the precise prediction of and control over the amount of peptide being delivered by regulating the amount of microspheres used. For an equal amount loaded, FITC-Comb1 showed the highest release levels, followed by biotinylated-Comb1. It is interesting that biotinylated-Comb1 showed lower levels of release compared to FITC-Comb1, considering that they are essentially the same peptide except for the tags with which they are functionalized. This trend was confirmed by the cumulative percentage released as compared to initial loading that was calculated for each peptide. Both peptides have a molecular weight of 3000 Da, which eliminates the possibility that the difference in release profile is due to differences in molecular weight. It is possible, however, that interactions between the biotin tag and the silk fibroin slowed the release of biotinylated-Comb1 from the microspheres, although this has not been described in the literature.

UN3-loaded microspheres showed the lowest levels of peptide release, suggesting that either UN3 had even stronger interactions with the silk fibroin than biotinylated-Comb1, or that not as much was successfully loaded into the microspheres. It is difficult to determine the extent of UN3's interaction with silk fibroin as it is a novel peptide that has never before been characterized in the literature. However, it would be useful to track the UN3 peptide total loading and loss throughout the microsphere process in the same way that was done for FITC-Comb1 in order to determine how much of the peptide is actually being loaded into the microspheres. Additionally, the molecular weight of UN3 is 2500 Da, which is lower than that of biotinylated-Comb1 and FITC-Comb1. However, in a study designed to

determine the effect of molecular weight on peptide release from silk films, Hofmann *et al.* showed that slower release rates from silk film correlate with higher molecular weights (2006). This suggests that since UN3 is the lighter peptide, it should be released faster compared to biotinylated-Comb1 and FITC-Comb1. However, this was not the observed trend.

Additional studies were performed in order to determine the stability of the encapsulated peptides in storage at 4 °C. Microspheres were stored for 7.5 months and then a four-day release study was performed comparing them to newly synthesized microspheres. FITC-Comb1 spheres showed no significant change in release between the old and new spheres. Biotinylated-Comb1, on the other hand, showed a logarithmic release profile for the new microspheres but a linear, near-zero release profile for the old microspheres. This suggests that the peptide, or at least its biotin tag, is degraded during the long term storage at 4 °C. It could be postulated that the biotinylated-Comb1 did not load into the old microspheres, but this is not supported since the tube proliferation study data in Figure 7 shows that release solution from biotinylated-Comb1 microspheres stimulated a greater level of tube proliferation than the control, albeit not to a statistically significant extent. This suggests that the microspheres were, at one time, loaded with bioactive biotinylated-Comb1 which later underwent degradation in storage. Finally, old UN3 microspheres showed a release profile that still fit a logarithmic regression curve but was reduced compared to the new UN3 microsphere release profile. Since detection of UN3 corresponds to anti-UN3 antibodies binding to a specific epitope on the peptide, reduced detection of the peptide implies that some of the protein was denatured in storage. Overall, these findings suggest that even lyophilized and stored at 4 °C, silk microspheres do not entirely protect the peptides from degradation over time.

The ELISA optimization study that was carried out for biotinylated-Comb1 and UN3 was able to successfully establish an effective protocol for assays for both peptides. For biotinylated-Comb1, a

streptavidin-HRP concentration of 0.5 µg/mL was chosen due to the linearity and high correlation ( $R^2 = 0.9889$ ) of its standard curve. For UN3, a number of different combinations of primary and secondary antibody concentrations were tested. Several curves fit a logarithmic regression curve with a correlation  $R^2 > 0.85$ , and of those, the one with the best correlation ( $R^2 = 0.9648$ ) was chosen for subsequent ELISA runs. This curve established 50 µg/mL as the appropriate primary antibody concentration and 1:500 as the secondary antibody dilution for the UN3 indirect ELISA. Development of these protocols is important for novel peptides like biotinylated-Comb1 and UN3, as it will allow them to be more easily quantified in solution, a requirement for many *in vitro* assays.

Equally as important as establishing an *in vitro* release profile for UN3, biotinylated-Comb1 and FITC-Comb1 microspheres was ascertaining that the peptides retained their biological activity after being released. In order to do this, an *in vitro* endothelial morphogenesis assay was performed on BREC cultured on Matrigel. The first assay was done in eight well glass chamber slides. At six hours post-plating, cells treated with the 25 nM UN3 microsphere release solution, 10 ng/mL bFGF, 100 nM Comb1 and 100 nM Comb1 combined with 25 nM UN3 all showed significantly greater tube proliferation than the 1% DMEM control. Although all three microsphere release solutions stimulated an increase in tube proliferation, only UN3 showed a statistically significant increase. The reason for this may be because the release solutions were stored at -20°C for several weeks before use. Although UN3 is relatively stable in solution, biotinylated-Comb1 and FITC-Comb1 may begin to undergo degradation after approximately one week in solution (Dr. Tatiana Demidova-Rice, personal communication), which may have undermined their potency.

However, the discrepancy between tube proliferation in the 25 nM UN3 microsphere release condition and the 25 nM UN3 condition is truly unexpected. These two conditions should be fairly equivalent, barring degradation due to processing of the microspheres, which would negatively impact

the UN3 release solution and not the stock UN3. It is unclear why the UN3 release solution was more bioactive than the stock UN3 at the same concentration. Furthermore, the situation is reversed at the 23 hour time point (Figure 9), although both treatments show lower proliferation than the control at that time.

The data for the 23 hour time point in this study are surprising in that most of the treatments, with the exception of 10 ng/mL bFGF, show tube proliferation that is significantly lower than the control treatment. Although the experimental release solutions were in DPBS, this was compensated for by diluting the DMEM control with DPBS to the same extent as well as adding extra BCS to both the control and experimental conditions. However, control UN3 and Comb1 were diluted in 1 M Tris (pH=8.0), which may have increased the osmolality of the media. Since mammalian cells require an osmolality range between 260 and 350 mOsm/kg (Invitrogen 2011), adding 1 M Tris to the growth media may have put a stress on the cells, counteracting the stimulation for tube proliferation by the positive controls. All three microsphere release solutions stimulated significantly lower tube proliferation than the control, indicating that they had lost their bioactivity. Again, this may be due to the protracted period of storage the solutions were subject to before use.

The main concern with the first tube proliferation study, however, was the fact that the effects of the microspheres themselves could not be measured. As shown in Figure 8 (F), microspheres aggregated on the surface of the cells, making it impossible to quantify how much tube proliferation had occurred. In order to address this, as well as some of the other shortcomings of the previous trial, the second trial was conducted in transwell plates coated with a thin layer of Matrigel at the bottom of each well. All controls, experimental solutions and microspheres were added to the transwells to isolate them from the cells. Furthermore, a larger volume of media was used, which meant that a smaller fraction of

the total media volume was either 1 M Tris or DPBS. This minimized the adverse effects of those solutes on the trial. Finally, a lower magnification was used for imaging to obtain a larger sample size.

Quantification of endothelial sprouts at 5 hours post-plating revealed high levels tube formation for the three microsphere groups, with biotinylated-Comb1, FITC-Comb1, and UN3 microspheres showing a 5.2, 6.1, and 8.1 fold increases compared to the control. Additionally, all of the positive controls showed significantly higher levels of tube proliferation than the 1% DMEM control, with 100 nM Comb1 being the highest at a 7.2 fold increase. These results show that the peptide being released by the microspheres are bioactive and affect stimulation of endothelial morphogenesis in BRECs. It should be noted that the increase in tube proliferation compared to the control reported here is much higher than that reported by Demidova-Rice *et al* (2011). This is probably because an equal number of initially plated cells were exposed to a higher volume of the same concentrations of peptides, which means that the peptides would not be depleted as rapidly in this assay as in the chamber slide tube proliferation assay.

At the 23 hour mark for the second assay, tube proliferation evened out across most of the experimental categories, with only the positive controls and the FITC-Comb1 spheres stimulating significantly greater tube proliferation. This is unsurprising, considering the reduced amount of Matrigel present in this assay. Figure 14 (B) – (E) shows tube formation in the positive controls and the FITC-Comb1 microsphere condition, showing the field fairly saturated with endothelial sprouts. This may indicate that the reason that tube proliferation leveled off between the different experimental groups was that the cells simply ran out of space for further tube proliferation, allowing the control group to catch up.

## Conclusions

Our first aim of describing the release profiles of microspheres loaded with UN3, biotinylated-Comb1, and FITC-Comb1 was successfully achieved. These profiles were fit to logarithmic regression curves with high correlation and can be used to predict peptide release from the silk microspheres at time points within the range they cover. Release was also calculated as a percentage of peptide initially loaded in order to help estimate the efficiency of the delivery system. The loading to release statistic was highest for FITC-Comb1, reaching 22% over a 14-day release period, and lowest for UN3, reaching a mere 3.7% over the same time period. Finally, a pilot study was conducted to track FITC-Comb1 loss throughout the microsphere synthesis process. Because our findings did not account for 100% of the peptide loss, it may be beneficial to determine an alternative to dissolving silk residue and microspheres in HFIP, as this may be damaging the peptide. Finally, this study should be extended to both UN3 and biotinylated-Comb1.

The aim of establishing the bioactivity of peptides released by the silk microspheres was also achieved. In the second tube proliferation study, all three microsphere-encapsulated peptides showed high, significant increases in tube proliferation compared to the control. However, it may have been beneficial to obtain another time point before the 23 hour mark, at which time there appeared to be a saturation of cells with tube-like structures.

Finally, an ELISA protocol was successfully established for the future quantification of biotinylated-Comb1 and UN3 in solution. Both Comb1 and UN3 are promising angiogenesis-stimulating peptides, and this study provides groundwork for future *in vitro* studies with these peptides as well as a characterization of their activity in the context of a silk microsphere drug delivery system.

## Future Work

This investigation found that the bulk of the microsphere-encapsulated peptide load was released within the first one to three days of the release profile studies. In order to improve the system's potential as a clinical drug delivery tool that would require a minimal frequency of re-administration, it would be advantageous to explore the possibility of extending the timeline of the release profile. In other microsphere systems, such as PLGA and alginate microspheres, it has been shown that the addition of silk coatings to the surface of the microspheres retards the release of peptides from the microspheres (Wang *et. al*, 2007). Eleanor Pritchard *et. al* (2010) have also shown that drug release from a solid powder reservoir system can be delayed by coating the reservoir with layers of silk fibroin. The same paper further showed that a delay in release can be affected by the concentration of silk used (increased concentration lead to an increased delay) and by post-coating methanol treatment. In the experiment described, methanol treatment caused an increase in  $\beta$ -sheet formation in the silk fibroin, which was thought to reduce the water permeability of the construct and thus slow the rate of drug release (Pritchard *et. al*, 2010). Thus, the first step for future work would be to explore the efficacy of additional silk fibroin coats, use of a higher silk solution concentration in microsphere formation, and longer treatment with methanol in order to extend the release timeline of the microspheres. Even if sustained, linear release could not be obtained, it would be possible to use a combination of regular and delayed-release microspheres to mimic linear release by insuring that as release from one set is ending, the other set is beginning to release the drug. Furthermore, coating the microspheres with silk fibroin could allow for the introduction of a second drug, for example an antiseptic, which would be released first and whose effects would synergize well with the effects of Comb1 and UN3.

A simultaneous next step for future work would be an *in vivo* trial of the drug delivery system. Current *in vivo* trials of Comb1 and UN3 are already underway in the Herman laboratory (Sackler School, Tufts University) using carboxymethyl cellulose (CMC) as the delivery vehicle, and show promise in stimulating angiogenesis. Since this study established the release profiles of silk microspheres loaded with biotinylated-Comb1, FITC-Comb1, and UN3, and further showed that the peptides retained their bioactivity throughout the processing, the next step is to carry out *in vivo* trials using this drug delivery mechanism. In addition, it is important to establish whether the microspheres can be added to the wound bed dry and hydrated on site, or whether they should be dissolved and injected immediately before use. Once the delivery system is fine-tuned and the safety and efficacy of the peptides is established, it is probable that this chronic wound healing system will become a serious contender in clinical trials due to its ease of administration, its potential for wholesale production (since it does not rely on isolating any elements from individual patients) and its ability to last a long time after every administration due to controlled release, which would minimize patient non-compliance issues. Overall, the combination of these peptides with the silk microsphere drug delivery system establishes a solid foundation for future innovation in chronic wound care.

## Literature Cited

Bristow, J., et al. "Tenascin-X: A Novel Extracellular Matrix Protein Encoded by the Human XB Gene Overlapping P450c21B." *The Journal of cell biology* 122.1 (1993): 265-78. Print.

Demidova-Rice, Tatiana N., Anita Geevarghese, and Ira M. Herman. "Bioactive Peptides Derived from Vascular Endothelial Cell Extracellular Matrices Promote Microvascular Morphogenesis and Wound Healing in Vitro." *Wound Repair and Regeneration* 19.1 (2011): 59-70. Web.

Egging, D., et al. "Wound Healing in Tenascin-X Deficient Mice Suggests that Tenascin-X is Involved in Matrix Maturation rather than Matrix Deposition." *Connective Tissue Research* 48.2 (2007): 93-8. Web.

Falanga, Vincent. "Wound Healing and its Impairment in the Diabetic Foot." *The Lancet* 366.9498 (2005): 1736-43. Print.

Hofmann, S., et al. "Silk Fibroin as an Organic Polymer for Controlled Drug Delivery." *Journal of Controlled Release* 111.1-2 (2006): 219-27. Print.

Ikuta, Tomoki, Hiroyoshi Ariga, and Ken-ichi Matsumoto. "Extracellular Matrix Tenascin-X in Combination with Vascular Endothelial Growth Factor B Enhances Endothelial Cell Proliferation." *Genes to Cells* 5.11 (2000): 913-27. Print.

Invitrogen, Inc. "Troubleshooting Cell Culture." (2011)Web.

Kleinman, Hynda K., and George R. Martin. "Matrigel: Basement Membrane Matrix with Biological

- Activity." *Seminars in cancer biology* 15.5 (2005): 378-86. Print.
- NCBI. FBN1 Fibrillin 1 [ Homo Sapiens ]. Gene ID: 2200 Vol. Bethesda, MD: National Center for Biotechnology Information, U.S. National Library of Medicine, 2011. Entrez Gene. Web.
- NCBI. TNXB Tenascin XB [ Homo Sapiens ]. Gene ID: 7148 Vol. Bethesda, MD: National Center for Biotechnology Information, U.S. National Library of Medicine, 2011. Entrez Gene. Web.
- Numata, Keiji, and David L. Kaplan. "Silk-Based Delivery Systems of Bioactive Molecules." *Advanced Drug Delivery Reviews* 62.15 (2010): 1497-508. Print.
- Page, Jeffrey C. "Critiquing Clinical Research of New Technologies for Diabetic Foot Wound Management." *The Journal of Foot and Ankle Surgery* 41.4 (2002): 251-9. Print.
- Pfaff, Martin, et al. "Cell Adhesion and Integrin Binding to Recombinant Human Fibrillin-1." *FEBS letters* 384.3 (1996): 247-50. Print.
- Pritchard, Eleanor M., et al. "Silk Fibroin Encapsulated Powder Reservoirs for Sustained Release of Adenosine." *Journal of Controlled Release* 144.2 (2010): 159-67. Print.
- Sottile, Jane. "Regulation of Angiogenesis by Extracellular Matrix." *Biochimica et Biophysica Acta (BBA) – Reviews on Cancer* 1654.1 (2004): 13-22. Print.
- Tatsioni, Athina, et al. "Usual Care in the Management of Chronic Wounds: A Review of the Recent Literature." *Journal of the American College of Surgeons* 205.4 (2007): 617,624.e57. Print.
- Wang, Xiaoqin, et al. "Silk Coatings on PLGA and Alginate Microspheres for Protein Delivery."

Biomaterials 28.28 (2007): 4161-9. Print.

Wenk, Esther, Hans P. Merkle, and Lorenz Meinel. "Silk Fibroin as a Vehicle for Drug Delivery

Applications." Journal of Controlled Release 150.2 (2011): 128-41. Print.